Experimental studies and simulation of laser ablation of high-density polyethylene films

by

Sandeep Ravi Kumar

A thesis submitted to the graduate faculty

in partial fulfillment of the requirements for the degree of

MASTER OF SCIENCE

Major: Industrial Engineering

Program of Study Committee:
Hantang Qin, Major Professor
Beiwen Li
Matthew Frank

The student author, whose presentation of the scholarship herein was approved by the program of study committee, is solely responsible for the content of this thesis. The Graduate College will ensure this thesis is globally accessible and will not permit alterations after a degree is conferred.

Iowa State University

Ames, Iowa

2020

DEDICATION

I dedicate my thesis work to my family and many friends. A special feeling of gratitude to my loving parents Ravi Kumar and Vasanthi, whose words of encouragement have made me what I am today.

TABLE OF CONTENTS

LIST OF FIGURES

LIST OF TABLES

Page

NOMENCLATURE

q_a	Ablative heat flux
q_i	General inward heat flux
h	Heat transfer coefficient
T	Temperature on the substrate at time t
T_a	Ablation temperature
Ramp	Ramp coefficient
V	Ablation velocity
Q	Cumulative heat flux
H_s	Heat of sublimation
LA	Laser ablation
HDPE	High-density polyethylene

ACKNOWLEDGMENTS

ABSTRACT

This thesis lays the groundwork for a simulation model for the laser ablation of polymer materials. A thorough review of the laser ablation of various polymer materials has been provided. The current trends and challenges in utilizing laser ablation for micro/nano manufacturing and information essential to the choice of an appropriate laser source for a polymer material have been provided. Experimental studies on laser ablation-based drilling of micro-holes on high-density polyethylene films have been performed. The influence of an increasing number of pulses and laser power on the depth and area of the micro-holes has been analyzed. The experimental results were utilized to validate a quantitative area-depth approximation model that was formulated based on the gain factors and the laser intensity profile. Additionally, a finite element method-based model has been developed for predicting the surface temperature and depth profile evolution with time during laser ablation of polymer materials.

CHAPTER 1.   GENERAL INTRODUCTION

1.1 Overview

Micro/nano-scale manufacturing has gained an increasing amount of attention and research interest in the past decade. There are several applications of micro/nano manufacturing in the medical and electronics fields like Micro Electro-Mechanical Systems (MEMS), micro-stents, catheters, and nano material fabrication.   These micro/nano-scale applications have many advantages, such as low power consumption products and wearable technology. Conventional machining techniques such as drilling, milling were adopted into the micro-scale to achieve features in the micrometer regime. However, there were several disadvantages to manufacturing micro/nano features using conventional techniques. For example, the tooling for creating such tiny features requires high precision and is expensive. Also, machining hard to machine materials such as titanium alloys with such tool sizes was complicated and needed frequent tool change. To overcome these challenges of conventional machining processes, advanced novel techniques were developed for the fabrication of features on the micro/nano-scale. Laser-based drilling, milling were some of the methods that were utilized to achieve machining on the micro-scale. All these laser-based manufacturing processes have a universal principle: Laser Ablation. Laser ablation is a top-down process of material removal. Under ideal conditions, the material to be removed is vaporized (sublimation) by a focused heat source. This process occurs only when the substrate absorbs a sufficient amount of energy. This meant that it was essential to choose optimum laser parameters for different material sources. For instance, certain materials have a good absorption coefficient at specific wavelengths, like polymers laser ablation work well with an ultraviolet laser source. Also, different materials have different ablation threshold fluence values, so the selection of proper power density is also a contributing factor. Although the principle of laser ablation is the

same, the mechanism by which it occurs depends on the above factors. For example, the ablation mechanism can be a purely thermal process, photochemical process, or a combination of both. Even though this novel method was capable of producing geometries in the micro/nano-scale, there were still several issues in terms of the quality and precision of the features produced. For example, achieving high aspect ratio features, avoiding re-deposition of the debris onto the substrate, and minimizing the Heat Affected Zone (HAZ) such that it does not affect the morphology of the material are some commonly faced challenges. These challenges called for the appropriate selections of laser parameters to avoid implications while employing laser ablation. However, experimentally determining the optimum setting by trial and error requires time and wastage of materials. To overcome this issue in determining the optimum parameters for laser ablation, a simulation model that can predict dimensions of the feature produced for a given set of laser parameters.

In this chapter, laser ablation experiments have been conducted on High-Density Polyethylene (HDPE) substrate, and the influence of laser parameters such as the number of pulses and power on the dimensions of the ablation crater has been established. Based on the experiments, a simple but effective approach to model micro-drilling process on HDPE substrates using pulsed laser ablation has been demonstrated and validated against additional experimental results. A sequential procedure used to establish this model has been provided, which would act as the knowledge base for adopting this model for laser ablation on other materials. In addition, a finite element method based numerical simulation models of continuous laser ablation of HDPE has been established using COMSOL to identify the temperature at the ablation surface and the ablation depth profile evolution over time. This model will pave the way for a better understanding of the ablation threshold conditions and identifying the ablation initiation in any material, given

the material properties are known. The models presented in this thesis will help predict the dimensions of the ablated holes or features for a given material and laser properties. This will help avoid the time and expenditure caused while determining the optimum laser parameters using the trial and error method.

1.2 Thesis Organization

This thesis consists of five chapters. Chapter 1 provides an overview of the research and motivation for conducting the research. Chapter 2 has a detailed literature review about laser ablation, its mechanism, and parameters. Additionally, the applications and issues with the ablation process have been presented. Chapter 3 contains the experimental setup, results, and discussion of the influence of laser pulse number and power on the area and depth of the ablated crater. Additionally, a quantitative model has been developed to predict the ablation depth and area of high-density polyethylene films. Chapter 4 focusses on the development of a preliminary FEM based laser ablation simulation model that predicts the surface temperature and depth profile evolution with time. This work will be an initial groundwork for a more sophisticated model for the prediction of the ablated surface. Chapter 5 will summarize the thesis work, the contributions along with the potential challenges, and future works of polymer laser ablation.

CHAPTER 2.   LASER ABLATION OF POLYMERS: A REVIEW

Modified from a manuscript published in Polymer International.

Sandeep Ravi-Kumar[a] , Benjamin Lies[a] , Xiao Zhang[a] , Hao Lyu[b] , Hantang Qin[a]

[a]Industrial and Manufacturing Systems Engineering, Iowa State University, Ames, IA 50011

USA; [b]College of Mathematics and Physics, Qingdao University of Science & Technology,

Shandong, China

I have contributed to more than 60% to the literature review paper titled "Laser Ablation of Polymers: A Review." I read through several research articles and journal papers on laser ablation of polymers and came up with a database of the type of laser sources used for different polymer materials and for different applications. This review article has been published on a top journal in the field of polymers "Polymer International" (https://onlinelibrary.wiley.com/journal/10970126).

2.1 Abstract

Laser ablation (LA), which employs a pulsed laser to remove materials from a substrate for generating micro/nano-structures, has tremendous applications in the fabrication of metals, ceramics, glasses, and polymers. It has become a noteworthy approach for achieving various functional structures in engineering, chemistry, biology, medicine, and other fields. Polymers are one such class of materials; they can be melted and vaporized at high temperatures during the ablation process. A number of polymers have been researched as candidate substrates in LA, and many different structures and patterns have been realized by this method. The current states of research and progress are reviewed from basic concepts to optimal parameters, polymer types, and applications. The significance of this paper is to provide a basis for follow-up research that leads to the development of superior materials and high-quality production through LA. In this review

chapter, we first introduce the basic concept of LA, including mechanism, laser types (millisecond, microsecond, nanosecond, picosecond, and femtosecond) and influential parameters (wavelength, repetition rate, fluence, and pulse duration). Then, we focus on several commonly used polymer materials and compare them in detail, including the effects of polymer properties, laser parameters, and feature designs. Finally, we summarize the applications of various structures fabricated by LA in a variety of areas along with a perspective of the challenges in this research area. Overall, a thorough review of LA of several polymers is presented, which could pave the way for the characterization of future novel materials.

2.2 Introduction

The laser is the acronym for "light amplification by stimulated emission of radiation," typically a high-intensity beam of electromagnetic radiation. The initial idea of laser theory was presented by Einstein [1]. However, the first ruby laser was developed in the year 1960 by the physicist Theodore H. Maiman. Soon after laser's experimental realization, there were several practical applications such as in the military, health, industrial, and scientific fields. The first widely recognized application of laser was laser printers, which were invented in 1971 by an American engineer Gary Starkweather [2]. There are significant applications of laser in manufacturing sectors like laser drilling [3], laser cutting, holography, laser metal deposition, and laser additive manufacturing [4,5].

Conventional machining techniques such as drilling, welding, milling, and turning are all capable of machining a wide variety of materials. However, it is difficult to achieve the best results in terms of surface finish and aspect ratio in machining hard-to-machine materials such as titanium [6] and superalloys [5]. These requirements in the industries led to the development of novel machining processes such as laser beam milling [7,8], laser drilling [3], and laser etching [8,9].

All of these lasers involved machining operations share a common phenomenon known as laser ablation.

Laser ablation is the top-down process of removing material by focusing a laser beam onto a substrate. Ablation occurs when the material absorbs sufficient energy to be melted or vaporized. The first instance using laser ablation was reported in 1965 by Smith for the deposition of thin films [10], but the films had poor quality due to ineffective experimental process control. Since then, the development and understanding of laser ablation have been incremental.

Laser ablation is widely used in the fabrication of metals, ceramics, glasses, and polymers. Polymers are of great interest due to the unique properties such as lightweight, corrosion resistance, lower frictional properties, less wear in comparison to metals [11], and their application potentials. In recent years, polymer-based laser ablation has gained huge interests due to its ability to be used for the fabrication of microfluidic channels [12], optical waveguides [13], and flexible electronics. The first report on the laser ablation of polymers was by Cozzens 1977 [14]. He used an infrared laser source (λ=10.6μm) to irradiate eleven different polymers. Since then, there has been a rapid rise in the applications of polymers such as nozzles for inkjet printers [15] and multi-chip modules [16]. Consequently, researchers started exploring the various aspects of using laser ablation for processing polymeric materials for such applications. For instance, researchers studied the influence of laser types and parameters on the accuracy and precision of the ablated features on the polymer materials. In this thesis, different laser types (see table 1) and the influences of laser parameters on ablated structures were reviewed.

Furthermore, we reviewed several common polymer materials used for laser ablation, including Polytetrafluoroethylene (PTFE), Polyimide (PI), Polydimethylsiloxane (PDMS), Polyethylene Terephthalate (PET) and Polymethyl Methacrylate (PMMA). The feature structures,

laser dependence, and properties were compared among those polymers. The review of laser ablation was based on the research activities of different groups, which can show the general development of this manufacturing method and give an outlook of it. It could pave the way for further development and application of laser ablation.

2.3 Laser Ablation

2.3.1 Mechanisms of Laser Ablation

The general mechanism of laser ablation is consistent throughout laser machining applications such as laser beam milling, high precision drilling, and laser cutting. Ablation is a combination of both vaporization and melt expulsion, as represented in Figure 2.1. When a focused beam of laser radiation strikes a surface, the electrons present in the substrate are excited by laser photons [17]. This excitation results in the generation of heat by absorbing photon energy, which is consistent with Beer Lambert's law [17, 18]. Beer Lambert's law states that the amount of light absorbed is dependent on the thickness of the materials and intensities of the light source. The heating effects cause melting or vaporization of the material, thus resulting in the removal of macroscopic materials from the substrate. The transition from solid to gas results in the formation of a plasma plume.
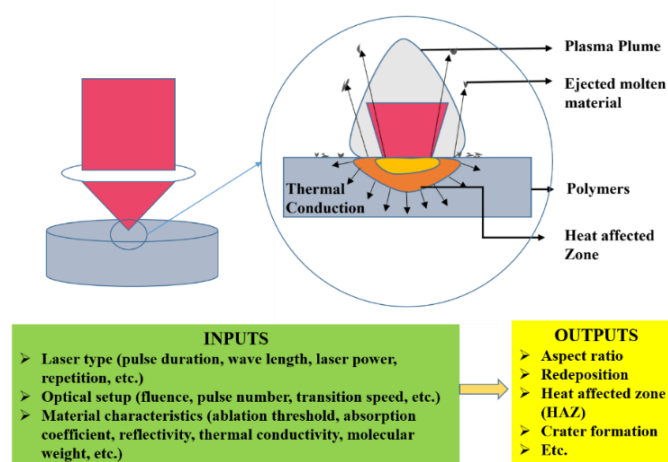
Figure 2.1 Laser-material interaction zone and input/output parameters

The transition from solid to the gaseous phase takes place in a series of steps. The initial heat produced by the absorption of the laser photons results in the formation of a melt pool at the laser-substrate interaction zone. The temperature further increases due to the incoming pulses, and the melt pool reaches the vaporization state [19]. High pressure is created during vaporization, which is also called a recoil pressure, which pushes molten materials from the pool where it is ejected [20]. The ejected material is a concern due to its re-deposition on the substrate. Also, it interacts with the incoming laser pulses [21, 22]. By further increasing the temperature at the laser-substrate interaction zone, the liquid attains an explosive liquid-vapor phase transition stage [23, 24]. The above mechanism is commonly seen during ablation using long-pulsed lasers. In this mechanism, the dynamics of the fluid phase and the vapor conditions are quite complex, and the re-solidification of the molten material also results in geometric changes in the ablated features.

Based on the properties of laser and material such as fluence, absorption coefficient, reflectivity, wavelength, and pulse duration, the ablation mechanism can be purely chemical or thermal or a combination of both. Photochemical ablation occurs due to the breaking of the covalent bonds in the polymer chains via the energy of the UV photons. Photothermal ablation considers the electronic excitation by the UV photons to be thermalized, which then results in the breaking of the polymer bonds. Several researches have focused on explaining the mechanisms present at the laser-material interaction area by assuming one mechanism dominates and then simulating the dominant process [25,26,27]. These various mechanisms are all dependent on the specific combination of light and material properties. As a result, it is essential to consider certain vital phenomena while studying the laser-material interaction. These phenomena include the type and magnitude of light energy absorption and the time scale of the laser pulse. The extreme intensity of the laser pulse in the ultra-short time frame provides inaccurate predictions under

classical heat transfer conditions. At normal intensities, the absorption is linear and follows Beer Lambert's law. This implies that the excited electrons by the photon absorption transfer the heat to the lattice, thereby resulting in melting and vaporization. However, at ultrashort timescale, the absorption becomes nonlinear and becomes intensity dependent. The bound electrons of the material can be directly ionized by the more intense absorption due to high intensities. So it is essential to characterize the laser being used and to predict the mechanism occurring at the laser-material interaction zone. These various mechanisms are all dependent on the specific combination of light and material properties. In practice, there are limitations regarding which combinations can be achieved, which is explained in the following sections.

2.3.2   Ablation Parameters

In order to better study polymer laser ablation, it is essential to understand the parameters involved in laser ablation of polymers, which depends on a variety of factors such as laser wavelength [28, 29], repetition rate [30], fluence [31], and pulse duration [32]. Firstly, for a laser system, there are two characteristics that are important to laser ablation, the monochromaticity, and directionality of the beam. The monochromaticity means that the wavelength of all emitted light is the same. This singular wavelength is very useful for calculations regarding the interaction of the light with optical components and material. The directionality of the beam refers to a low angle of divergence, and this increases the ease at which the light is controlled and focused. The effective optical spot size, directly related to laser fluence, is different for each system and plays a vital role in ablation. Here, the fluence is the total energy of the laser over the area represented by the focal spot size and is typically measured in J/cm2. The most common laser type used in the ablation process is the pulsed laser. In the case of a pulsed laser, it is appropriate to measure the fluence of each pulse as opposed to the fluence over the total time. These individual pulses can vary in duration and in repetition rate and are characteristic of the laser type, which will be discussed in

the next section. The positioning of the focal spot of the laser on the substrate influences the etch rate, redeposition of the debris, and the microstructures formed on the sample surface [33]. The research conducted by Wang reported easier machining and lesser debris redeposition while focusing the laser near the bottom surface of the sample [34]. Lei studied the backside and front side ablation of a gold film on a silicon substrate under varying pulse energies and focal positions [35]. He accounts for the presence of two types of damage happening based on the laser fluence: Ablation and Burst. He used Finite Element Method (FEM) simulation to verify the burst damage occurring during the backside ablation.

In addition to the influence of the laser source, properties of the substrate materials such as thermal conductivity [36], absorption coefficient [37], and reflectance [38] will all influence the ablation structures as well. Despite the fluence of the laser being used, the absorption of photons by the material is essential for ablation to happen. Each material has unique absorption coefficients for different beam wavelengths. For example, polymers generally exhibit increased absorption of the photons at ultraviolet wavelengths. Once the light has been absorbed by the material, it is important to consider how the surrounding material is affected by the transfer of heat through thermal conductivity. The molecular weight of the polymer also influences the ablation efficiency [39]. It has been reported that the increase in molecular weight results in a highly viscous molten material during ablation and consequently results in a lower ablation rate of the polymer [39].

The combination of these material characteristics and the optical properties of the incident light result in various ablation mechanisms. The emphasis on which mechanism to focus on is dependent on the application of the light/material interaction. The focus of this review is the laser ablation of polymers, all of which emphasize the same general mechanism. The ideal output

characteristics of these mechanisms include high aspect ratios, limited heat affected zone, minimal material redeposition, and better minimum resolution on polymers.

2.3.3 Laser Source

The laser sources can be classified based on their wavelengths into Ultraviolet/Excimer Lasers and Infrared Lasers. An excimer laser is a pulsed gas laser that emits UV light with a power efficiency between 0.2% and 2% [40]. Excimer laser gained attraction because most polymers exhibit a high absorption coefficient at excimer wavelengths and the ease of making a small portion of laser to strike on to the work surface using an aperture [41]. Typical examples of excimer laser are F_2 laser, ArF laser, KrF laser, XeCl laser, and CeBr laser having an emission wavelength in the ultraviolet spectrum (10 to 400 nm) [40]. A drawback of using excimer lasers for ablation purposes is that the gas used as the laser medium has to be changed more frequently. As a substitute for these excimer lasers, a diode-pumped solid-state laser such as Nd: YAG lasers are used [42, 43]. They are capable of achieving the ablation threshold at small spot sizes because of high-quality beams. Still, it is difficult to mask the laser without forming diffraction patterns on the irradiated surface. The other way to classify laser sources is based on the timescale of their pulse durations. The lasers are classified into millisecond (ms, 10^{-3}s), microsecond (μs, 10^{-6}s), nanosecond (ns, 10^{-9}s), picosecond (ps, 10^{-12}s), and femtosecond (fs, 10^{-15}s) lasers. The timescales of the laser pulses influence the ablation mechanism, accuracy, and precision of the features. Millisecond and microsecond lasers are produced by chopping the continuous wave laser beam. It has been reported that the ablation of polymers by long pulses, leaves evidence of molten materials and carbonization of the walls of the ablated features [44]. Unlike longer laser pulses, ultrashort laser pulses in the timescales of femtoseconds or picoseconds provide advantages in terms of high precision, large material removal rate, and minimal thermal damage. It is attributed to two processes: thermal diffusion and nonlinear absorption. In the ultrashort timescale, there is

insufficient time to transfer the heat energy from the excited electrons to the lattice, causing minimal thermal damage. However, under extreme intensities, the plasma plume generated tends to result in heating of the surrounding material. This minimization in energy loss due to thermal diffusion helps achieve features with high aspect ratios, no recast layer, and minimal cracking [45].

2.4 Polymer Material

Laser parameters and material properties both affect the success of laser ablation. Aside from researches on the creation of the laser beams, the materials themselves have been heavily researched and studied. In this section of the thesis, the review is focusing on polymer materials and their related ablation processes. Research has been conducted on polymer materials that have promising applications in various fields such as medical, engineering, and chemical sensing. The materials required of these fields limit the composition and, thus, the material characteristics that are integral to performing laser ablation.

The polymers used for laser ablation have been classified based on several criteria, such as their availability, application, ablation behavior, and decomposition behavior. For example, Polymethyl Methacrylate (PMMA) depolymerizes upon irradiation while polyimides (PI) decompose into fragments upon irradiation. Similarly, certain polymers are available readily, such as PMMA, PET, and PTFE, whereas some are customized based on specific requirements of the application (Designed Polymers). Certain polymers such as PDMS and Polycaprolactone are used in biomedical applications such as venal implants and cell encapsulation. A summary of polymers and related laser sources are listed in Table 2.1.

Table 2.1. Types of polymer ablated corresponding to different laser sources

Polymer	Laser Sources
Polymethyl Methacrylate (PMMA)	KrF laser [52,53,54,55], Nd: YAG laser [56], ArF [54,57,58], KrCl [54], XeCl [44,59], CO_2 [44]
Polystyrene (PS)	KrF laser [52], ArF laser [60,61]
Poly(α-methyl styrene)	ArF [58]
Polyimide (PI)	XeCl [62, 63, 64, 65, 66, 67], ArF laser [66,67,68], KrF laser [52,62,66,67,68,69], XeF laser [68], Nd: YAG laser [70,71], KrCl laser[64], Nd: YVO_4 [72]
Polyethylene Terephthalate (PET)	ArF laser [58,73], KrF laser [52], XeCl [63]
Bisphenol Polycarbonate (BP PC)	ArF laser [58], KrF laser [52,74]
Polyethylene (PE)	Iodine PALS [75]
Polytetrafluoroethylene (PTFE)	KrF laser [52,76]
Polyether Ether Ketone (PEEK)	XeCl laser [77], KrF laser [78], Nd:YAG [79], Nd:YVO_4 [80,81], CO_2 [82]
Polyacetylene	ArF laser [72]
Polydimethyl Glutaramide (PMGI)	XeCl laser [44,83]
Polyetherimide (PEI)	ArF laser [84], XeCl laser [84], KrF laser [84], Nd:YAG [85]
Nylon	XeCl laser [86], Nd:YAG [86,87], CO_2 [86]
Polydimethylsiloxane (PDMS)	CO_2 laser[88,89], Ti:sappire laser [90], ArF laser [91], Erbium doped fiber laser [92]

2.4.1   Polytetrafluoroethylene (PTFE)

Polytetrafluoroethylene (PTFE), also known as Teflon, is a crystalline synthetic fluoropolymer of tetrafluoroethylene. Teflon, with an absorption coefficient of 158 cm^{-1}, is a weak absorber. It is a highly versatile material used in a wide variety of applications owing to its stability and durable characteristics. Due to its good electrical resistance, it is used as an insulator for wiring and cables. PTFE is used in mechanical engineering applications in parts that have sliding action such as gears and pulleys since they have a low frictional coefficient. PTFE is widely used in the

food packaging industry and in the chemical industry as a material for sealing aggressive chemicals. As mentioned previously, each application requires different material characteristics. This leads to the creation of several grades of PTFE based on the filler material incorporated into it. Venkateshwarlu studied the effects of various fillers on the mechanical properties of PTFE based composites [87]. He used glass, bronze, carbon, mica, sand, porcelain, alumina, antimony trisulphide, and marble as fillers and studied the mechanical properties, including hardness and tensile strength.

With the versatility in the properties of PTFE for different grades, PTFE has been successfully applied in the medical and electronics sector. For example, membranes of PTFE are used as a barrier for bone promotion around titanium implants [88]. These applications involve the material to have features in micro/nano-scale and demand precision. Researchers investigated the methods to minimize defects, such as the heat-affected zone and surface dendrite formation. Kuper studied the ablation of PTFE with femtosecond UV laser pulses at 248 nm [46]. He reported that thermal damage was absent for fluences as low as 0.5 J/cm^2 with an ablation rate of 1 µm per pulse.

Womack studied the use of femtosecond laser ablation in depositing thin films of PTFE on silicon wafers [70]. She emphasized that the femtosecond (fs) lasers produced precisely machined features, unlike nanosecond laser pulses. The deposition rate and film quality were characterized by using scanning electron microscopy, X-ray diffraction, and IR spectroscopy, which showed strong supports of high deposition and quality by using fs laser pulses. Huber studied the ablation rate of sintered PTFE and reported its dependence on the wavelength of the laser [89]. He reported that, at a given laser fluence value, the ablation rate increased initially and then decreased as the wavelength increased. He further stated that there was no relationship between the experimentally

measured ablation depth and the linear optical penetration depth, which was calculated using a Monte Carlo simulation. Mitra measured the laser ablation threshold of PTFE using a photothermal beam deflection technique [90]. He measured the ablation threshold at different wavelengths and estimated the coefficient of absorption of Teflon at each wavelength. He reported that the value of the absorption coefficient increases with a decrease in wavelength. Wang investigated the laser ablation of PTFE in ambient air [91]. He reported the clear edge definition and increase in ablation depth can be achieved by increasing the number of pulses. The effect of air ionization at higher fluences in deteriorating the ablated structure quality and decreasing the ablation efficiency was reported. While all other researches were focused on ablating pure PTFE, there have been researches that focused on identifying the advantage of doping PTFE. Yang said the ablation of PTFE doped with aluminum nanoparticles [92]. He stated that the doped Teflon can be ablated precisely with near infrared laser and does not require a vacuum ultraviolet or femtosecond excimer laser.

2.4.2   Polyimide (PI)

Polyimide is a high-temperature engineering plastic. Polyimides are thermally stable even up to the temperature range of 300-400 ˚C. As a result of its high heat and fire resistance compared to other polymer materials, PI is suitable for a diverse range of applications such as aerospace, optoelectronics, and defense. They have good machinability, electrical, and thermal insulation properties [93].

The machining efficiency and etching mechanism of polyimides via laser ablation have been investigated. Brannon studied etching of polyimide using pulsed excimer lasers of different wavelengths (248, 308, 351 nm) [56]. He reported that the laser ablation threshold at which significant etching occurred can be correlated with the wavelength-dependent absorption coefficient. It was stated that the absorbed energy per unit volume required to etch the substrate is

equal for several distinct wavelengths. It is reported that the presence of oxygen does not influence the etch rate, but it controls the oxidation of the ablated material. Yu, Ma, and Lei conducted laser ablation of molybdenum (Mo) on the polyimide substrate using the axicon lens [94]. They studied the narrow grooves produced by ablation under varying parameters such as laser power, scanning speed, and the axicon tip distance from the sample. Selective scribing of the Mo material on the PI substrate was attributed to the large difference in threshold fluence of Mo and PI ($0.18J/cm^2$ and $0.75J/cm^2$ respectively at 60 fs pulse duration). They reported that the use of an axicon focused beam could produce narrow groves of high quality even with large height fluctuations of moving substrates.

Research has been conducted to determine the influence of laser parameters such as pulse duration and pulse repetition rate on the ablation of polyimides. Taylor used photoacoustic spectroscopy to determine the dependence of pulse duration on the ablation of polyimide using a XeCl laser source [57]. He ablated PI with XeCl laser of pulse duration 7-300 ns and reported that the ablation threshold has a weak relation with the pulse duration. He observed an etch depth of 0.1-1 µm per laser pulse, and it was independent of the pulse duration. However, there are other processes that occur during the laser ablation of PI at particular pulse durations. Chuang studied the laser ablation of PI using Nd: YAG laser (355 nm) to investigate the saturation of the ablation rate with an increase in laser fluence [64]. He reported 80 percent saturation at the fluence of 0.5 mJ/cm^2. He measured the reflectivity, emission intensity, and photoacoustic signal based on the fluence values. It was concluded that the trailing part of the laser pulse was blocked by the plasma plume and the excited polymer particles, which prevented the laser from hitting the polymer substrate.

Apart from saturating the ablation rate, the debris formed has been found to have an influence on the morphology of the ablated polymers. Taylor studied the distribution of the ablated debris formed during the XeCl laser (308 nm) ablation of pure and dopant induced PI [58]. Similar to Dyer [95] and Niino [96], Taylor observed cone-like structure formation on the surface of both polymers. He reported that the cone formation was due to the redeposition of the debris and not based on impurities in the polymer.

2.4.3 Polydimethylsiloxane (PDMS)

PDMS is a mineral-organic polymer belonging to the siloxane family. The structure of the PDMS consists of carbon and silicon. PDMS has been widely used in the fabrication of microfluidic devices. It is used as a food additive and as an anti-foaming agent in beverages. One reason to use PDMS to manufacture microfluidic devices is its transparency at optical frequencies, which allows for visibility of the contents in the micro-channel. Additional reasons include its autofluorescence [97], bio-compatibility, and inexpensiveness compared to the previously used materials such as silicon.

Researchers studied the use of laser ablation with PDMS to manufacture microfluidic devices of different features in a cost-efficient manner. Yan studied the use of laser ablation techniques to produce single-layer microfluidic devices with abrupt depth variations [82]. He used the laser to engrave channel patterns on to PMMA plate and then used it to create the master pattern for the single-layer PDMS microfluidic devices. He reported the capability of this technique to produce microfluidic devices with micrometer structures in one step. Li reported a simple, cost-effective method for fabricating microfluidic devices with PDMS multilayer configurations [83]. He used a system similar to Yan and used conventional lithography, and sputtering technique to fabricate an alignment bonding of top and bottom electrode patterned substrates. This was used for the integration of the electronics in the microfluidic devices. He further validated the proposed

method by fabricating and testing a di-electrophoresis based integrated electronic microfluidic chip for the manipulation of microparticles. Wolfe studied Ti:Sapphire laser (femtosecond pulses) to produce stamps for micro-contact printing and for the fabrication of microfluidic channels [84]. This proposed technique was capable of producing features as small as 1 µm in width and 2 µm in pitch. Unlike conventional molding, this technique does not need curing.

Unlike using a mask for fabricating the PDMS micro-channels, researchers focused on identifying methods for direct fabrication of the microchannels on polymer materials. Hautefille reported a technique to etch microscale volumes of material from the PDMS surface [98]. He utilized infrared laser along with microscopic clusters of carbon materials to generate microplasma at the PDMS-air interface layer. Further, he reported the technique's application to fabricate interesting photonic features and the presence of combustion residues in the form of carbon nano domains with local fluorescence and increased hydrophobicity. Hsieh studied the direct micromachining of microfluidic channels on PDMS and other biodegradable materials such as polyglycerol sebacate [85]. He proposed a polymer surface modification method for the fabrication of a microfluidic system, which eliminated the steps of mask/mold production as in photolithographic or soft photolithographic techniques. He also investigated the relationship between laser parameters, depth, and width of the ablated features.

Another research topic in the field of laser ablation of PDMS is direct micro patterning and fabrication. Huang studied the thin-layer separation and micro-fabrication of PDMS using an ultra-short pulsed IR laser (1552 nm) [86]. The influence of pulse overlap rate and irradiation pulse energy on the ablation width, depth, and surface quality are analyzed. He reported a pulse overlap rate range of 1-2 pulses per µm and 1-1.5 µJ to achieve quality separation and fabrication without any visible thermal damages. Moon studied the effect of crater size on the surface morphology of

PDMS [99]. He studied the PDMS surface with varying both the interpulse interval and the inter-spot distance between successive pulses. It was reported that the surface morphology was dependent both on the inter-spot distant and interpulse interval between successive pulses.

2.4.4 Polyethylene Terephthalate (PET)

PET is a commonly used transparent thermoplastic in the textile industry as polyester, packaging industry, and as an engineering plastic when combined with other materials such as glass fiber to improve the material strength. There have been numerous studies on the application of laser ablation for micromachining of PET and the mechanism occurring at the laser-material interaction zone. Watanabe studied the fragmentation of PET during laser ablation using a 248 nm excimer pulse to characterize the ablation mechanism [81]. He reported that the fragmentation was accelerated by thermal energy at fluence above the threshold value of 30 mJ/cm2. He stated the importance of both thermal and photochemical reactions in the ablation of PET. Other defects on laser ablating PET are studied by investigating the surface of the substrate. Arenholz studied the surface of PET after irradiation by an ultraviolet laser at various wavelengths (193 nm, 248 nm, 308 nm) to better understand the growth and structure of surface dendrites using atomic force microscopy [100]. He reported that the size (length of dendrite arms) and structure of the dendrite were dependent on the laser wavelength and the ambient pressure. By studying the surface of PET after ablating with 193 nm ArF laser [67], Lazare reported an increase in surface roughness as the number of laser pulses increased. The surface roughness peaked at a maximum of 1-2 μm at ten pulses.

There were researchers who tried to understand the contribution of laser ablation on the morphological changes in the material. Mansour studied the surface-induced morphology changes on ablating PET using Nd: YAG laser of 266 nm [101]. He proposed a theoretical model to determine the ablation etch depth for a given incident laser fluence. P.E. Dyer studied the excimer

laser ablation of PET and reported the thermal coupling and etch rate measurements and observed that a thermal balance was present up to the threshold fluence and above which the ablated material removed excess energy [61].

The influence of laser parameters such as pulse width and wavelength on the ablation efficiency and surface morphology have been investigated. Liu studied the difference between the use of short and long pulses for the ablation process [102]. He used a Ti: sapphire laser source to ablate PET. He reported that the heat-affected zone, cracks, and non-uniform ablation were more frequent during ablating with a higher pulse width (200 ps) as opposed to a shorter pulse (80 fs). With the increasing interest in the identification of the cause of defects, researchers started to investigate methods to control defect growth during laser ablation. Elaboudi studied the photoablation of polymers underwater and compared it with ablation in the air [103]. He reported that the threshold fluence decreases while ablating underwater and aimed at identifying the hydrolysis reaction responsible for the decrease in laser threshold.

2.4.5 Polymethyl Methacrylate (PMMA)

PMMA is another type of low-cost thermoplastic, also known as acrylic glass. It is widely used in applications such as optical, biomedical, solar, sensors, and nanotechnology. There have been numerous studies geared toward understanding the application of laser ablation for machining PMMA. Specifically, how the precision and resolution (aspect ratio, recast layer, re-deposition, micro-cracks) are affected by the laser as well as the material properties (absorption coefficient and thermal conductivity). Nayak studied the effects of laser power and processing speed on the precision of the depth, width, and surface profiles of microchannels manufactured on PMMA of different polymer weights (96.7 kDa, 120 kDa, 350 kDa, and 996 kDa) using a CO2 laser [39]. He observed that the depth and width increase along with laser power. There were pores formed in higher molecular weight PMMA, whereas none were observed in lower molecular weight samples.

He reported that the choice of material was the key factor for CO2 laser ablation for applications that require high precision.

Similarly, Baudach studied the precision of the width and depth of features machined on PMMA films of 250 μm using Ti: sapphire laser. He observed that the ablation threshold value varied between 0.5-2.5 J/cm^2 depends on the number of laser pulses hitting the spot. He reported that the diameter of holes (μm) was influenced by the laser fluence and the number of pulses [104]. Beyond studying the precision of the machined features, researchers paid great attention to device fabrication and testing. Klank reported the ease of producing microfluidic channels in PMMA using CO^2 laser. He reports that the feature depth can be controlled by the laser power and scanning speed [105]. The Gaussian beam created during LA has been verified to help for self-aligning the optical fibers.

Although laser ablation, under the proper control of parameters, is capable of producing micro/nano-scale features with precision and accuracy, there are a considerable amount of defects such as a recast layer, redeposition of debris, and heat-affected zone. Researchers have studied the ablated debris to better understand the photochemical reactions occurring and the process by which the debris is ejected and then redeposited. Danielzik [51, 53] and Estler [50] used quadrupole mass spectrometry to study the ablated particles. Estler studied the photochemical composition of the ablated particles and reported the change in the composition with varying wavelengths. Danielzik studied the velocity distribution of the ablated PMMA particles and reported it to change between thermal velocity distribution and non-Maxwellian velocity distribution depending on the laser fluence. Burrell [52] used X-ray photoelectron spectroscopy to study PMMA and Poly(α-methyl styrene) surface composition after irradiating it with a laser in the UV wavelength. He reported the

absence of surface compositional changes, which indicated that no surface intermediates that are different from the starting materials were formed.

The formation of craters around the ablated surface is another defect that has been investigated. Efthimiopoulos studied XeCl laser ablation of weakly absorbing PMMA and reported the formation and collapse of bubbles [106]. He stated that the phenomenon of bubble creation and collapse occurs over multiple pulses while using 3-9 J/cm^2 energy fluence. For high energy fluence (>9 J/cm^2), the bubble creation and collapse occur with a single pulse duration. He concluded that successive pulses might be needed to advance the process of bubble creation and collapse based on the energy fluence.

There are other applications of PMMA, such as thin film deposition and nano particle generation. Blanchet studied the deposition of thin films of PMMA by laser ablation using Nd: YAG laser in the ultraviolet wavelength range [107]. He reported that the temperature of the substrate was important to determine the morphology and molecular weight of the films. The films were maintained at temperatures between 100 and 200 ˚C. The deposition occurred due to the ejected monomer falling on the glass substrate and redeposited due to the re-polymerization of the monomers.

2.4.6   Other Polymers

There are several other polymers that have been studied for laser ablation. Polyetherimide (PEI), a high-temperature resistant thermoplastic, is used for the production of PEI embossing tools. These tools are used for the packaging of membranes and the production of microchannels for the use of sealing bosses [79]. It was reported that the boss width was dependent on the laser diameter. Jensen studied the use of laser ablation for the rapid prototyping of microsystems made of polymers [72]. He created a microsystem using Polyether ether ketone (PEEK), which can be

used for injection molding a series of prototypes. He stated that this application could be extended to other thermally and mechanically strong polymers such as PEI.

Polyethersulfone (PES) is another polymer that has been widely used as a replacement for metals in automotive components. Similar to other polymers, researchers studied the mechanism that leads to the formation of these micro defects on the surface of the films. Laser-induced surface microstructure formation was first reported by Dyer [95]. Niino observed the formation of microstructures on the surface of PES films while ablating with a XeCl laser source [96]. He studied the mechanism resulting in the formation of these microstructures using a XeF laser source. He reported that the thermal processes on the ablated surface played a significant role in the formation of the microstructures.

Although laser ablation of polymers was first reported in 1965, it was not possible to fully exploit the potential of polymer laser ablation using the commercially available polymers such as PMMA, PI, PTFE, PET, PEI, PES, PE, and PDMS. This was because of the drawbacks of these polymers, such as carbonization, ablation debris re-deposition, and low sensitivity to laser radiation. This led to the idea of designed polymers: synthesizing polymers based on specific requirements of applications. The basic idea behind this approach is to combine the properties of one polymer with others. For example, Triazene polymers tend to have high etch rates and good ablation quality but poor stability (oxidation of the substrate during irradiation). On the other hand, Polyesters exhibited higher stabilities but poor sensitivities (absorption at particular wavelengths). A designed polymer aimed at combining these two polymers in order to achieve high-quality machining (high surface finish, less heat affected zone, and high aspect ratio).

Similar to other commercially available polymers, researches have been conducted to understand the ablation mechanism, their efficiency, and the defects that arise during their

application. The impact of structural parameters on the ablation behavior and characteristics has been studied. Triazo based polymers are one class of designed polymers that contain triazene chromophore in its polymer chain. Lippert studied the laser ablation of triazene polymers films (50 μm thick) using PI as a reference polymer [108]. He measured the etch rates, threshold fluence, and the surface defects induced during laser ablation. He reported that the polymers containing the triazene group have the lowest ablation threshold fluence (25 mJ/cm^2) and the highest etch rate (3 μm/pulse). Lippert further investigated the triazene group polymer's laser ablation to identify the influence of etch depth per pulse on the laser fluence [109]. The complete absence of debris was attributed to the photolysis reaction that decomposes the fragments. It was concluded that the removal of material from areas larger than the laser beam was due to the generation of shock waves while irradiated with high fluence laser pulses.

The dynamic behavior of the etching process was also investigated. Hauer studied the ablation of triazene group polymers and PI reference films using XeCl (308 nm) and ArF lasers (193nm) using nano second interferometry and shadowgraphy [110]. Similar to Lippert [108], he reported the absence of surface swelling and the presence of a shock wave. He reported the etching of triazene polymer to start and stops with the laser beam. The speed of shock waves to increase with an increase in fluence and was higher for 193 nm than 308 nm wavelength laser beams.

Another class of designed polymers is the diazo based polymers. They exhibit excellent absorption at 308 nm wavelengths. Similar to triazo based polymers, these polymers contain a diazo chromophore in its polymer chain. Some of the examples of diazo based polymers are diazo sulfide polymer, diazo sulfonate polymer, and diazo phosphonate polymer. Jeffers studied the use of the diazo coating in the preparation of printing plates by irradiating with laser light [111]. Busman invented a process of laser-induced mass transfer imaging of materials using diazo

compounds [112]. He emphasized that the new method will improve the sensitivity of the laser-induced thermal imaging with the use of diazo compounds.

2.5 Applications of Laser Ablation of Polymers

The application of laser ablation on polymers extends over a broad spectrum. The phenomena of laser ablation have been used in the LIGA process, which is a combination of lithography, electroplating, and molding. This process is typically used to create a pattern that is then used for mass fabrication. The most commonly used polymer in the LIGA process is PI [113]. PI is coated over a silicon wafer substrate where laser ablation is then utilized to create micro features with high aspect ratios on the polymer material. Once the features have been formed on the polymer, electroplating is done to coat the polymer surface with metals [113]. Subsequent to the metal deposition, the polymer material can be dissolved, resulting in the shell created by the metal coating. Because of PI's high thermal stability and insolubility in most solvents, there is difficulty in stripping it off after electroplating. Current research in this field is aimed at developing novel polymer materials that can meet the requirements of the laser LIGA process.

Another widely used application of laser ablation is in the field of telecommunication. Fiber Bragg gratings (FBG) in the telecommunication field require the outer layer of polymer material to be removed in addition to the actual "inscription" on the fiber optics when obtaining side written gratings [114]. Some of the traditional ways of achieving this are by means of mechanical stripping or chemical stripping. But there are disadvantages of using these techniques such as structural damages and environmental effects. Laser ablation for removal of the material has been found to overcome the limitations of traditional methods [115]. Further, researchers are investigating laser ablation for jacket stripping of single-mode fiber (SMF), which has a dual polymer layer system [116].

Laser ablation of polymeric materials has been extensively used in the fabrication of high-performance photonic devices, micro fluidic devices, and optical waveguides. It has been reported that laser ablation can produce clean vertical cuts through plastics and polymer waveguide core [117]. This technique has been found to provide efficient coupling of light from optical fibers into polymer photonic devices. One example will be the fabrication of micro lenses. A KrF excimer laser was scanned over successive contours of chosen diameter and scanning velocity. An array of lens was fabricated based on the aperture used for shaping the laser beam. Naessens reported the method for micro lens fabrication in polycarbonate material utilizing an excimer laser [118]. Pan said the laser ablation of PI for the fabrication of polymeric micro-optical components [119]. This method of fabrication of micro lenses provides flexibility in terms of shape, focal length, and diameter of the lenses.

The field of micro-electro-mechanical systems (MEMS) have also adopted laser ablation. Lan reported the fabrication of MEMS on silicon and PI substrate by laser ablation using a 355 nm laser source [120]. He was able to manufacture microscopic holes and nozzles of various diameters using low power laser direct drilling. This fabrication technique is fast and clean compared to a traditional photolithography process.

Laser ablation has been used in the medical field for the fabrication of biomedical devices for the use in minimally invasive surgery and other advanced surgical techniques. Laser ablation and other micromachining techniques help achieve the complex and small feature sizes required in these devices. In addition to the fabrication tools and devices for surgical application, the laser ablation technique is directly used for surgery of the cornea. Trokel reported the use of excimer laser for removal of the corneal tissues in cow eyes [121]. The laser-tissue interaction was photochemical in nature. He also told of the absence of thermal damage to the adjacent tissues.

2.6 Challenges and Future Scope

Although laser ablation of polymers has been researched for the past two decades, there are still several challenges that have yet to be addressed. For instance, there are several models and simulations that try to explain the ablation mechanism at the laser-material interaction zone that results in the etching of the material. These models tend to explain the physics phenomenon such as absorption, reflectivity, optical excitation, thermal, and chemical reactions to refer to the ablation occurring at the laser-material interaction. However, it is difficult for a systematic way to explain the ablation mechanism of these phenomena. Some models assume the ablation occurs purely due to thermal reactions occurring due to laser irradiation, while other models suggest chemical reactions are dominant. A single model cannot explain the ablation in different materials because the mechanism of ablation depends on the type of laser and the properties of the material. Future research is needed in studying the contribution of each physical phenomena in etching the material and investigating an optimal model that accurately explains the ablation mechanism from a system point of view.

Micro/nano manufacturing requires high-quality control of the material, precision, accuracy, and process during laser ablation. Despite the extensive study on laser ablation of a variety of polymers and understanding the influence of laser parameters and material properties on the ablation, there are inaccuracies in machining a feature of desired dimensions. Currently, it is difficult to create a feature of the exact desired depth and width. This is because of phenomena such as heating of the substrate over subsequent pulses, plasma plume formation, and etch debris interfering with the subsequent pulses. Presently, there is no perfectly accurate physical model that helps in determining the optimal parameter for synthesizing the desired feature dimension. Future research focusing on establishing a quantitative model that can improve the parameter settings

(spot size, repetition rate, pulse duration, intensity) required to achieve the desired dimension will contribute to increasing the application of laser ablation to various fields.

Further research in studying laser ablation of composite polymer materials would be of great scope. The use of fiber-reinforced composites has become more common due to the strength and lightweight of the material. Along with the growing use of composites, the need for composite repair and machining is growing as well. Traditional machining processes have trouble with fiber-reinforced composites due to the abrasive nature of the combination. Ablation may have great potential in that area as it has been used in the past to ablate fused silica (glass fibers) and various polymers in the past.

2.7 Summary and Outlook

Laser ablation has become a powerful method in the fabrication of micro/nano structures on various polymers. The discussions provided in the previous sections are an overview of the works done in the field of laser ablation over the past two decades for polymer-based laser ablation. The effect of laser parameters on machining, their influence on the substrate's surface morphology, and the various applications of laser ablation have been studied. These parameters are dependent on both the material composition as well as the laser characteristics. Different laser types and influences of laser parameters to ablated polymeric structures have been reviewed. Several common polymer materials, including Polytetrafluoroethylene (PTFE), Polyimide (PI), Polyethylene Terephthalate (PET), Polydimethylsiloxane (PDMS) and Poly Methyl Methacrylate (PMMA) are analyzed in the effects of polymer properties, laser parameters, and feature designs. The review of laser ablation is based on the research activities of different groups and can show the general development of this manufacturing method.

Several overarching trends have been observed throughout this review. While these trends can be used for a preliminary understanding of laser ablation, a deeper understanding should be derived from the works being reviewed.

- Smaller pulse duration results in more vaporization and less melting. Higher Melting can cause a large HAZ and redeposition due to expulsion, cracks, and non-uniformity. Also, more vaporization results in the formation of a plasma plume, which can reduce the quality of the ablated features due to saturation.

- The absorption coefficient of a given material varies for different wavelengths. This needs to be well characterized in order to make any accurate predictions. This means that the combination of laser type and material used is very important.

- A high repetition rate may not leave enough time for the plasma to disperse during vaporization, thus reducing the effectiveness of successive pulses due to interference.

- Higher molecular weight can result in lower ablation rates due to the formation of highly viscous molten material during ablation.

- Larger thermal conductivity of a material can lead to a larger HAZ, specifically with longer pulse durations.

As the development of modern manufacturing based on laser ablation, the coming years will see the further development of LA towards a precise controlling technology with many applications beyond polymers. Quantitative verification and the modeling of laser ablation are quite complex and can always be further improved. In addition to the study of the mechanisms of ablation, precision, accuracy, and process control can also be enhanced from a manufacturing point of view. Future research into establishing a quantitative model that can suggest the parameter

settings (spot size, repetition rate, pulse duration, intensity) required to achieve the desired dimension will increase the applicability of laser ablation in various fields.

2.8 Chapter 2: References

[1] Einstein, A. (1917). Zurquantentheorie der strahlung.Phys. Z.,18, 121-128.

[2] Townes, C. H. (2010). The first laser Charles H. Townes.A Century of Nature: Twenty-One Discoveries that Changed Science and the World, 107.

[3] Larsson, I. F. (1968).U.S. Patent No. 3,410,979. Washington, DC: U.S. Patent and Trademark Office.

[4] Akinlabi, Esther Titilayo, Rasheedat Modupe Mahamood, and Stephen Akinwale Akinlabi, eds. (2016) Advanced Manufacturing Techniques Using Laser Material Processing. IGI Global, 2016

[5] Bogue, R. (2015). Lasers in manufacturing: a review of technologies and applications. Assembly Automation, 35(2), 161-165.

[6] Choragudi, A., Kuttolamadom, M. A., Jones, J. J., Mears, M. L., & Kurfess, T. (2010). Investigation of the machining of titanium components in lightweight vehicles. In SAE International Congress.

[7] Dubey, A. K., & Yadava, V. (2008). Laser beam machining—a review. International Journal of Machine Tools and Manufacture, 48(6), 609-628.

[8] Raymond, S., & Mueller, J. L. F. (1968).U.S. Patent No. 3,364,087. Washington, DC: U.S. Patent and Trademark Office.

[9] Chovan, J. L., & Manoni, A. J. (1975).U.S. Patent No. 3,920,951. Washington, DC: U.S. Patent and Trademark Office.

[10] Smith AH, Turner AF (1965) Appl Opt 4:147

[11] National Research Council. (1994). Polymer Science and Engineering: The Shifting Research Frontiers. National Academies Press.

[12] Becker, H., & Gärtner, C. (2000). Polymer microfabrication methods for microfluidic analytical applications. Electrophoresis, 21(1), 12-26.

[13] Van Steenberge, G., Hendrickx, N., Bosman, E., Van Erps, J., Thienpont, H., & Van Daele, P. (2006). Laser ablation of parallel optical interconnect waveguides. IEEE Photonics Technology Letters, 18(9), 1106-1108

[14] Cozzens, R. F., & Fox, R. B. (1978). Infrared laser ablation of polymers. Polymer Engineering & Science, 18(11), 900-904.

[15] Aoki H (04/1998). U.S. Patent 5736999.

[16] Patel RS, Wassick TA (1997) Proc SPIE-Int Soc Opt Eng 2991:217

[17] Brown, M. S., & Arnold, C. B. (2010). Fundamentals of laser-material interaction and application to multiscale surface modification. In Laser precision microfabrication (pp. 91-120). Springer, Berlin, Heidelberg.

[18] Ahmed, N., Darwish, S., & Alahmari, A. M. (2016). Laser ablation and laser-hybrid ablation processes: a review. Materials and Manufacturing Processes, 31(9), 1121-1142.

[19] Von der Linde, D., & Sokolowski-Tinten, K. (2000). The physical mechanisms of short-pulse laser ablation. Applied Surface Science, 154, 1-10.

[20] Hoffman, J. (2015). The effect of recoil pressure in the ablation of polycrystalline graphite by a nanosecond laser pulse. Journal of Physics D: Applied Physics, 48(23), 235201.

[21] Singh, S., Argument, M., Tsui, Y. Y., & Fedosejevs, R. (2005). Effect of ambient air pressure on debris re-deposition during laser ablation of glass. Journal of applied physics, 98(11), 113520.

[22] Tangwarodomnukun, V., Likhitangsuwat, P., Tevinpibanphan, O., & Dumkum, C. (2015). Laser ablation of titanium alloy under a thin and flowing water layer. International Journal of Machine Tools and Manufacture, 89, 14-28.

[23] Miotello, A., & Kelly, R. (1999). Laser-induced phase explosion: new physical problems when a condensed phase approaches the thermodynamic critical temperature. Applied Physics A, 69(1), S67-S73.

[24] Bulgakova, N. M., & Bulgakov, A. V. (2001). Pulsed laser ablation of solids: transition from normal vaporization to phase explosion. Applied Physics A, 73(2), 199-208

[25] Cain, S. R. (1993). A photothermal model for polymer ablation: chemical modification. The Journal of Physical Chemistry, 97(29), 7572-7577.

[26] D'couto, G. C., & amp; Babu, S. V. (1994). Heat transfer and material removal in pulsed excimer-laser-induced ablation: Pulse width dependence. Journal of applied physics, 76(5), 3052-3058.

[27] Mahan, G. D., Cole, H. S., Liu, Y. S., & amp; Philipp, H. R. (1988). Theory of polymer ablation. Applied physics letters, 53(24), 2377-2379.

[28] LaHaye, N. L., Harilal, S. S., Diwakar, P. K., Hassanein, A., & Kulkarni, P.(2013).The effect of ultrafast laser wavelength on ablation properties and implications on sample introduction in inductively coupled plasma mass spectrometry. Journal of applied physics, 114(2), 023103.

[29] Aguiar, R., Trtik, V., Sánchez, F., Ferrater, C., & Varela, M. (1997). Effects of wavelength,

deposition rate and thickness on laser ablation deposited YSZ films on Si (100). Thin Solid Films, 304(1-2), 225-228.

[30] Burns,F.C.,& Cain,S.R.(1996).The effect of pulse repetition rate on laser ablation of polyimide and polymethyl methacrylate-based polymers. Journal of Physics D: Applied Physics, 29(5), 1349.

[31] Okamuro, K., Hashida, M., Miyasaka, Y., Ikuta, Y., Tokita, S., & Sakabe, S. (2010). Laser fluence dependence of periodic grating structures formed on metal surfaces under femtosecond laser pulse irradiation. Physical Review B, 82(16), 165417.

[32] Chichkov, B.N., Momma, C., Nolte, S., VonAlvensleben, F., & Tünnermann, A. (1996). Femtosecond, picosecond and nanosecond laser ablation of solids. Applied Physics A, 63(2), 109-115

[33] Wang, W., Mei, X., Jiang, G., Lei, S., & Yang, C. (2008). Effect of two typical focus positions on microstructure shape and morphology in femtosecond laser multi-pulse ablation of metals. Applied Surface Science, 255(5), 2303-2311.

[34] Wang, Z. K., Seow, W. L., Wang, X. C., & Zheng, H. Y. (2015). Effect of laser beam scanning mode on material removal efficiency in laser ablation for micromachining of glass. Journal of Laser Applications, 27(S2), S28004.

[35] Lei, S., Grojo, D., Ma, J., Yu, X., & Wu, H. (2016). Femtosecond Laser backside Ablation of Gold Film on Silicon Substrate. Procedia Manufacturing, 5, 594-608.

[36] Pham, D., Tonge, L., Cao, J., Wright, J., Papiernik, M., Harvey, E., & Nicolau, D. (2002). Effects of polymer properties on laser ablation behaviour. Smart materials and structures, 11(5), 668

[37] Johnson, S. L., Schriver, K. E., Haglund Jr, R. F., & Bubb, D. M.(2009). Effects of the absorption coefficient on resonant infrared laser ablation of poly(ethylene glycol). Journal of Applied Physics, 105(2), 024901.

[38] Benavides, O., Golikov, V., & Lebedeva, O.(2013). Reflection of high-intensity nanosecond Nd: YAG laser pulses by metals. Applied Physics A, 112(1), 113-117.

[39] Nayak, N. C., Lam, Y. C., Yue, C. Y., & Sinha, A. T. (2008). CO_2-laser micromachining of PMMA: the effect of polymer molecular weight. Journal of micromechanics and microengineering, 18(9), 095020.

[40] Paschotta, R. (2008).Field guide to lasers (Vol. 12). SPIE press

[41] Speidell, J.L., Pulaski, D.P., & Patel, R.S. (1997).Masks for laser ablation technology: new requirements and challenges. IBM Journal of research and development, 41(1.2), 143-148.

[42] Chang, W.S., Shin, B., Kim, J.G.,& Whang, K.H.(2004).Photothermal three-dimensional fabrication of polymers using diode-pumped solid state lasers. Journal of

Micro/Nanolithography, MEMS, and MOEMS,3(3), 472-478.

[43] Dyer, P.E., Pervolaraki, M.,& Lippert, T.(2005).Experimental studies and thermal modelling of 1064- and 532-nm Nd: YVO4 micro-laser ablation of polyimide. Applied Physics A,80(3), 529-536.

[44] Srinivasan, R., Hall, R. R., Loehle, W. D., Wilson, W. D., & Allbee, D. C. (1995). Chemical transformations of the polyimide Kapton brought about by ultraviolet laser radiation. Journal of applied physics, 78(8), 4881-4887.

[45] Shirk, M. D., & Molian, P. A. (1998). A review of ultrashort pulsed laser ablation of materials. Journal of Laser Applications, 10(1), 18-28.

[46] Küper, S., & Stuke, M. (1987). Femtosecond UV excimer laser ablation. Applied Physics B, 44(4), 199-20

[47] Kawamura, Y., Toyoda, K.,& Namba, S.(1982).Effective deep ultraviolet photoetching of polymethyl methacrylate by an excimer laser. Applied Physics Letters, 40(5), 374-375

[48] Davis, G. M., & Gower, M. C. (1987). Time resolved transmission studies of poly (methyl methacrylate) films during ultraviolet laser ablative photodecomposition. Journal of applied physics, 61(5), 2090-2092.

[49] Dijkkamp, D., Gozdz, A. S., Venkatesan, T., & Wu, X. D. (1987). Evidence for the thermal nature of laser-induced polymer ablation. Physical review letters, 58(20), 2142

[50] Estler, R.C., & Nogar, N.S. (1986). Mass spectroscopic identification of wavelength dependent UV laser photo ablation fragments from polymethyl methacrylate. Applied physics letters, 49(18), 1175-1177.

[51] Danielzik, B., Fabricius, N., Röwekamp, M., & Von der Linde, D. (1986). Velocity distribution of molecular fragments from polymethyl methacrylate irradiated with UV laser pulses. Applied physics letters, 48(3), 212-214.

[52] Burrell, M.C., Liu, Y.S., & Cole, H.S. (1986). An x-ray photoelectron spectroscopy study of poly(methyl methacrylate) and poly(α-methyl styrene) surfaces irradiated by excimer lasers. Journal of Vacuum Science & Technology A: Vacuum, Surfaces, and Films, 4(6), 2459-2462.

[53] Masuhara, H., Hiraoka, H., & Domen, K. (1987). Dopant-induced ablation of poly (methyl methacrylate) by a 308-nm excimer laser. Macromolecules, 20(2), 450-452.

[54] Cole, H. S., Liu, Y. S., & Philipp, H. R. (1986). Dependence of photoetching rates of polymers at 193 nm on optical absorption depth. Applied physics letters, 48(1), 76-77.

[55] Feldmann, D., Kutzner, J., Laukemper, J., MacRobert, S., & Welge, K.H. (1987). Mass spectroscopic studies of the ArF-laser photo ablation of polystyrene. Applied Physics B, 44(2), 81-85.

[56] Brannon, J. H., Lankard, J. R., Baise, A. I., Burns, F., & Kaufman, J. (1985). Excimer laser etching of polyimide. Journal of Applied Physics, 58(5), 2036-2043

[57] Taylor, R.S., Singleton, D.L., & Paraskevopoulos, G. (1987). Effect of optical pulse duration on the XeCl laser ablation of polymers and biological tissue. Applied physics letters, 50(25), 1779-1781.

[58] Taylor, R.S., Leopold, K.E., Singleton, D.L., Paraskevopoulos, G., & Irwin, R.S. (1988). The effect of debris formation on the morphology of excimer laser ablated polymers. Journal of applied physics, 64(5), 2815-2818.

[59] Simon,P.(1989).Time-resolved ablation-site photography of XeCl-laser irradiated polyimide. Applied Physics B, 48(3), 253-256.

[60] Srinivasan, R., Braren, B., & Dreyfus, R.W. (1987).Ultraviolet laser ablation of polyimide films. Journal of applied physics, 61(1), 372-376.

[61] Dyer, P.E., & Sidhu, J.(1985). Excimer laser ablation and thermal coupling efficiency to polymer films. Journal of applied physics, 57(4), 1420-1422.

[62] Yeh, J.T.C.(1986). Laser ablation of polymers. Journal of Vacuum Science & Technology A: Vacuum, Surfaces, and Films, 4(3), 653-658.

[63] Koren, G.(1988). Plume temperature in the laser ablation of polyimide films measured by infrared emission spectroscopy. Applied Physics B, 46(2), 147-149.

[64] Chuang, M.C., & Tam, A.C. (1989). On the saturation effect in the picosecond near ultraviolet laser ablation of polyimide. Journal of Applied Physics, 65(7), 2591-2595

[65] Creasy, W. R., & Brenna, J. T. (1988). Large carbon cluster ion formation by laser ablation of polyimide and graphite. Chemical physics, 126(2-3), 453-468.

[66] Shin, B.S., Oh, J.Y.,& Sohn, H.(2007).Theoretical and experimental investigations into laser ablation of polyimide and copper films with 355-nm Nd: YVO4 laser. Journal of materials processing technology, 187, 260-263

[67] Lazare, S.,& Srinivasan, R.(1986).Surface properties of poly(ethylene terephthalate) films modified by far-ultraviolet radiation at 193nm (laser) and185nm (low intensity).The Journal of Physical Chemistry, 90(10), 2124-2131.

[68] Braren, B., & Srinivasan, R.(1985). Optical and photochemical factors which influence etching of polymers by ablative photo decomposition. Journal of Vacuum Science & Technology B: Microelectronics Processing and Phenomena, 3(3), 913-917.

[69] Torrisi, L., Gammino, S., Mezzasalma, A.M., Visco, A.M., Badziak, J., Parys, P., & Pfeifer, M.(2004). Laser ablation of UHMWPE-polyethylene by 438 nm high energy pulsed laser. Applied surface science, 227(1-4), 164-174.

[70] Womack, M., Vendan, M.,& Molian, P.(2004).Femtosecond pulsed laser ablation and deposition of thin films of polytetrafluoroethylene. Applied Surface Science, 221(1-4), 99-109.

[71] Dyer, P.E., Oldershaw, G.A., & Schudel, D.(1990). XeCl laser ablation of polyetheretherketone. Applied Physics B, 51(5), 314-316.

[72] Jensen, M. F., McCormack, J. E., Helbo, B., Christensen, L. H., Christensen, T. R., & Geschke, O.(2004). Rapid prototyping of polymer microsystems via excimer laser ablation of polymeric molds. Lab on a Chip, 4(4), 391-395.

[73] Romoli, L., Fischer, F., & Kling, R.(2012). A study on UV laser drilling of PEEK reinforced with carbon fibers. Optics and Lasers in Engineering, 50(3), 449-457.

[74] Riveiro, A., Soto, R., Comesaña, R., Boutinguiza, M.D., Del Val, J., Quintero, F., & Pou,J.(2012).Laser surface modification of PEEK. Applied Surface Science, 258(23), 9437-9442.

[75] Lasagni, A. F., Acevedo, D. F., Barbero, C. A., & Mücklich, F. (2007). One-Step Production of Organized Surface Architectures on Polymeric Materials by Direct Laser Interference Patterning. Advanced Engineering Materials, 9(1-2), 99-103.

[76] Sumiyoshi, T., Ninomiya, Y., Ogasawara, H., Obara, M., & Tanaka, H. (1994). Efficient ablation of organic polymers polyethersulphone and polyetheretherketone by a TEA CO2 laser with high perforationability. Applied Physics A, 58(5), 475-479.

[77] Hiraoka, H., Chuang, T. J., & Masuhara, H. (1988). Dopant-induced ablation of polymers by a 308 nm excimer laser. Journal of Vacuum Science & Technology B: Microelectronics Processing and Phenomena, 6(1), 463-46

[78] Liu, Y.S., & Grubb, W.T. (1989).U.S.Patent No.4,882,200. Washington, DC: U.S. Patent and Trademark Office

[79] Kim, G. D., Rundel, J. T., & Paul, B. K. (2010). UV laser ablation of polyetherimide embossing tools for the packaging of membranes and microchannel using sealing bosses. International Journal of Precision Engineering and Manufacturing, 11(5), 665-671.

[80] Skordoulis, C.D., Makropoulou, M., & Serafetinides, A.A. (1995). Ablation of nylon-6, 6 with UV and IR lasers. Applied surface science, 86(1-4), 239-244.

[81] Watanabe, H., & Yamamoto, M. (1997). Laser ablation of poly (ethylene terephthalate). Journal of applied polymer science, 64(6), 1203-1209.

[82] Yan, Z., Huang, X., & Yang, C. (2017). Rapid prototyping of single-layer microfluidic PDMS devices with abrupt depth variations under non-clean-room conditions by using laser ablation and UV-curable polymer. Microfluidics and Nanofluidics, 21(6), 108.

[83] Li, M., Li, S., Wu, J., Wen, W., Li, W., & Alici, G. (2012). A simple and cost-effective

method for fabrication of integrated electronic-microfluidic devices using a laser-patterned PDMS layer. Microfluidics and Nanofluidics, 12(5), 751-760

[84] Wolfe, D. B., Ashcom, J. B., Hwang, J. C., Schaffer, C. B., Mazur, E., & Whitesides, G. M. (2003). Customization of poly (dimethylsiloxane) stamps by micromachining using a femtosecond-pulsed laser. Advanced Materials, 15(1), 62-65.

[85] Hsieh, Y. K., Chen, S. C., Huang, W. L., Hsu, K. P., Gorday, K. A. V., Wang, T., & Wang, J. (2017). Direct Micromachining of Microfluidic Channels on Biodegradable Materials Using Laser Ablation. Polymers, 9(7), 242.

[86] Huang, H., & Guo, Z. (2009). Ultra-short pulsed laser PDMS thin-layer separation and micro-fabrication. Journal of Micromechanics and Microengineering, 19(5), 055007

[87] Venkateswarlu, G., Sharada, R., & Rao, M. B. (2015). Effect of Fillers on Di-electric Strength of PTFE Based Composites. International Journal of Scientific and Research Publications.

[88] Becker, W., Dahlin, C., Becker, B. E., Lekholm, U., Van Steenberghe, D., Higuchi, K.,& Kultje, C.(1994).The use of e-PTFE barrier membranes for bone promotion around titanium plants placed into extraction sockets: a prospective multicenter study. International Journal of Oral & Maxillofacial Implants, 9(1).

[89] Huber, N., Heitz, J., & Bäuerle, D. (2004). Pulsed laser ablation of polytetrafluoroethylene (PTFE) at various wavelengths. The European Physical Journal-Applied Physics, 25(1), 33-38

[90] Mitra, A., & Thareja, R. K. (1999). Determination of laser ablation threshold of Teflon at different harmonics of Nd: YAG laser using photothermal deflection technique. Journal of materials science, 34(3), 615-619

[91] Wang, Z. B., Hong, M. H., Lu, Y. F., Wu, D. J., Lan, B., & Chong, T. C. (2003). Femtosecond laser ablation of polytetrafluoroethylene (Teflon) in ambient air. Journal of applied physics, 93(10), 6375-6380.

[92] Yang, Y., Wang, S., Sun, Z., & Dlott, D. D. (2004). Near-infrared laser ablation of poly tetrafluoroethylene(Teflon) sensitized by nano energetic materials. Applied physics letters, 85(9), 1493-1495.

[93] Liaw, D.J., Wang, K.L., Huang, Y.C., Lee, K.R., Lai, J.Y., & Ha, C.S. (2012).Advanced polyimide materials: syntheses, physical properties and applications. Progress in Polymer Science, 37(7), 907-974.

[94] Yu, X., Ma, J., & Lei, S. (2015). Femtosecond laser scribing of Mo thin film on flexible substrate using axicon focused beam. Journal of Manufacturing Processes, 20, 349-355.

[95] Dyer, P.E., Jenkins, S.D., & Sidhu,J. (1986).Development and origin of conical structures on XeCl laser ablated polyimide. Applied Physics Letters,49(8), 453-455

[96] Niino, H., Shimoyama, M.,& Yabe, A.(1990).XeCl excimer laser ablation of a polyethersulfone film: Dependence of periodic microstructures on a polarized beam. Applied physics letters, 57(22), 2368-2370.

[97] Piruska, A. et al. The autofluorescence of plastic materials and chips measured under laser irradiation. Lab. Chip 5, 1348–1354 (2005).

[98] Hautefeuille, M., Cabriales, L., Pimentel-Domínguez, R., Velázquez, V., Hernández-Cordero, J., Oropeza-Ramos, L., & López-Moreno, E. (2013). New perspectives for direct PDMS microfabrication using a CD-DVD laser. Lab on a Chip,13(24), 4848-4854.

[99] Moon, H. Y., Sidhu, M. S., Lee, H. S., & Jeoung, S. C. (2015). Dynamic changes in PDMS surface morphology in femtosecond laser treatment. Optics Express,23(15), 19854-19862.

[100] Arenholz, E., Kirchebner, A., Klose, S., Heitz, J., & Bäuerle, D. (1998). Deposition of ablation products from UV-laser irradiated polymer surfaces. MRS Online Proceedings Library Archive, 526.

[101] Mansour, N., & Ghaleh, K.J. (2002). Ablation of polyethylene terephthalate at 266 nm. Applied Physics A, 74(1), 63-67.

[102] Liu, X., Du, D., & Mourou, G. (1997). Laser ablation and micromachining with ultrashort laser pulses. IEEE Journal of quantum electronics, 33(10), 1706-1716.

[103] Elaboudi, I., Lazare, S., Belin, C., Talaga, D., & Labrugère, C. (2008). Underwater excimer laser ablation of polymers. Applied Physics A, 92(4), 743-748.

[104] Baudach, S., Bonse, J., Krüger, J., & Kautek, W. (2000). Ultrashort pulse laser ablation of polycarbonate and polymethylmethacrylate. Applied surface science, 154, 555-560.

[105] Klank, H., Kutter, J. P., & Geschke, O. (2002). CO2-laser micromachining and back-end processing for rapid production of PMMA-based microfluidic systems. Lab on a Chip, 2(4), 242-246.

[106] Efthimiopoulos, T., Kiagias, C., Heliotis, G., & Helidonis, E. (2000). Evidence of volume bubble creation during laser ablation of PMMA organic polymer. Canadian Journal of Physics, 78(5-6), 509-519.

[107] Blanchet, G. B. (1995). Deposition of poly (methyl methacrylate) films by UV laser ablation. Macromolecules, 28(13), 4603-4607.

[108] Lippert, T., Dickinson, J. T., Hauer, M., Kopitkovas, G., Langford, S. C., Masuhara, H., & Tomita, K. (2002). Polymers designed for laser ablation-influence of photochemical properties.Applied surface science, 197, 746-756.

[109] Lippert, T., Stebani, J., Ihlemann, J., Nuyken, O., & Wokaun, A. (1993). Excimer laser ablation of novel triazene polymers: influence of structural parameters on the ablation characteristics. The Journal of Physical Chemistry, 97(47), 12296-12301.

[110] Hauer, M., Funk, D. J., Lippert, T., & Wokaun, A. J. (2002, September). Laser ablation of a triazene polymer studied by ns-interferometry and shadowgraphy. InHigh-Power Laser Ablation IV (Vol. 4760, pp. 259-269). International Society for Optics and Photonics.

[111] Jeffers, W., Seeley, D., Faust, R. J., & Liu, S. (1981).U.S. Patent No. 4,248,959. Washington, DC: U.S. Patent and Trademark Office.

[112] Busman, S. C., Cuny, G. D., Zaklika, K. A., & Ellis, R. J. (1997).U.S. Patent No. 5,691,098. Washington, DC: U.S. Patent and Trademark Office.

[113] Yang, C. R., Hsieh, Y. S., Hwang, G. Y., & Lee, Y. D. (2004). Photoablation characteristics of novel polyimides synthesized for high-aspect-ratio excimer laser LIGA process. Journal of Micromechanics and Microengineering, 14(4), 480

[114] Kashyap, R. Fiber Bragg Gratings. 1999

[115] Barnier, F., Dyer, P. E., Monk, P., Snelling, H. V., & Rourke, H. (2000). Fiber optic jacket removal by pulsed laser ablation. Journal of Physics D:Applied Physics, 33(7), 757.

[116] Snelling, H. V., Walton, C. D., & Whitehead, D. J. (2004). Polymer jacket stripping of optical fibers by laser irradiation. Applied Physics A, 79(4-6), 937-940

[117] Jiang, J., Callender, C. L., Noad, J. P., Walker, R. B., Mihailov, S. J., Ding, J., & Day, M. (2004). All-polymer photonic devices using excimer laser micromachining. IEEE Photonics Technology Letters, 16(2), 509-511.

[118] Naessens, K., Ottevaere, H., Baets, R., Van Daele, P., & Thienpont, H. (2003). Direct writing of micro-lenses in polycarbonate with excimer laser ablation. Applied Optics, 42(31), 6349-6359.

[119] Pan, C. T., & Shen, S. C. (2004). Design and fabrication of polymeric micro-optical components using excimer laser ablation. Materials science and technology, 20(2), 270-274.

[120] Lan, B., Hong, M. H., Kaidong, D. Y., Chen, S. X., & Chong, T. C. (2003, February). Laser ablation for MEMS microfabrication on Si and Kapton substrates. In Third International Symposium on Laser Precision Microfabrication (Vol. 4830, pp. 196-201). International Society for Optics and Photonics

[121] Trokel, S. L., Srinivasan, R., & Braren, B. (1983). Excimer laser surgery of the cornea. American journal of ophthalmology, 96(6), 710-715.

CHAPTER 3.   AN AREA-DEPTH APPROXIMATION MODEL OF MICRO-DRILLING ON HIGH-DENSITY POLYETHYLENE (HDPE) SOFT FILMS USING PULSED LASER ABLATION

Modified from a manuscript published in the Journal of Micro and Nano Manufacturing.

Sandeep Ravi-Kumar[a] , Xiao Zhang[a], Benjamin Lies[a], Hao Lyu[b], Hantang Qin[a]

[a]*Industrial and Manufacturing Systems Engineering, Iowa State University, Ames, IA 50011 USA; [b]College of Mathematics and Physics, Qingdao University of Science & Technology, Shandong, China*

My research has been focused on establishing simulation models to predict ablation profiles better and to help develop a better understanding of the polymer laser ablation. I have conducted experiments on polymer laser ablation of HDPE and developed a quantitative model to predict the dimensions of micro drilled holes. This work is published in the "Journal of Micro and Nano-manufacturing" titled "An Area-Depth Approximation Model of Micro-drilling on High-Density Polyethylene Soft Films Using Pulsed Laser Ablation" (https://doi.org/10.1115/1.4045331). I have contributed to more than 70% of the works presented in this chapter.

3.1 Abstract

Micro-drilling based on laser ablation has been widely applied for manufacturing micro/nano features on different materials as a non-contact thermal removal approach. It has the advantages of high aspect ratio manufacturing capability and reduced surface damage. However, laser ablation is a complicated process that is challenging to model, thus manufacturing accuracy and dimensional prediction are essential yet difficult aspects when a new substrate material is tested. In this thesis chapter, a standardized modeling procedure was demonstrated to predict the area and depth of laser ablation based on experimental study and simulation validation. A case

study was conducted where micro-drilling of high-density polyethylene (HDPE) was investigated using a 1064nm nanosecond pulsed laser. Blind micro-holes were fabricated on the HDPE samples by ablating under different laser powers and the number of pulses. Gain factors were defined and determined by the experimental data. A quantitative area-depth approximation model was formulated based on the gain factors and the Gaussian laser intensity profile, which can predict the ablated dimensions on the HDPE samples and enhance the control of manufacturing accuracy. A comparison of the measured and the simulated results of micro-holes presented average 96.5% accuracy for the area and 85.7% for the depth. This research provided a simple but effective approach to predict dimensions of micro-holes on various substrates using laser ablation under different laser power and the number of pulses, which could pave the way for development and modeling of laser ablation on polymers.

3.2 Introduction

Laser ablation of polymers has been the area of considerable investigation over the past several decades. This is because of its potential applications in machining features in the micro-scale with minimal surface morphological changes [1]. Other notable uses of laser ablation of polymers are in the LIGA process to create patterns, fabrication of high-performance photonic devices [2, 3], optical waveguides micro-fluidic channels [4, 5] and micro-electro-mechanical systems [6]. Ablation is a subtractive process that combines both evaporations and melt expulsion. The ablation occurs when the material absorbs sufficient energy to be vaporized or melted. The absorbed energy from the laser photons results in the heating, melting, and vaporization of the substrate. In some cases, the substrate electrons excited by photons could result in the breakage of the covalent bonds in the polymer chains [7]. Also, there is a considerable amount of heat absorbed by the surrounding materials, resulting in heat-affected zones and thermal cracks. Despite the

extensive research on laser ablation, the interaction between the substrate and the laser beam has not been well understood, especially in the case of polymer laser ablation [8]. Polymer laser ablation involves both photo-thermal and photochemical reactions. It has been reported that the infrared radiation produced a photo-thermal reaction, while the ultraviolet wavelength produced photochemical reactions at the laser-material interaction zone [9].

In addition to the mechanism, the ablation process depends on several laser and material parameters (wavelength [10, 11], repetition rate [12], fluence, pulse duration [13], absorption coefficient [14], thermal conductivity [15] and reflectivity [16, 17]), which leads to the difficulty of universally predicting the process occurring at the laser-material interaction zone. Higher fluence generates improved ablation rate and resulting in increased heat affected zone [18]. The repetition rate of the laser influences heat accumulation and incubation in the substrate [12]. The vaporization of the material produces the formation of a plasma plume, which interferes with the incoming laser pulses. Thus, the absorption of a portion of the pulse energy and a reduction in the ablation rate is generated [19, 20]. Irrespective of the laser fluence, the amount of heat absorbed depends on the absorption coefficient of the substrate [14, 21]. Higher molecular weight polymers result in a decrease in ablation efficiency because of the formation of a highly viscous molten material [22]. In addition to the laser and the material properties, optical parameters such as the positioning and size of the focal spot of the laser on the substrate influence the ablation rate [23].

Several studies have been conducted on the ablation of polyethylene, and because of the above-mentioned ambiguities at the laser-material interaction, modeling of the ablation process has been a challenging task. Tawfik reported the ablated crater depth and mass of HDPE using laser-induced plasma spectroscopy technique and obtained the influence of the number of pulses

on the ablated depth [24]. Torrissi studied the laser ablation of ultra-high molecular weight polyethylene using a 438 nm laser and reported the influence of laser pulse energy on the ablated crater depth and volume [25]. Gordon established a finite element model that explained the thermal processes occurring at the laser-material interaction zone during the ablation of polyimide [26]. He also modeled the temperature dependence on the ablation rate and the influence of the laser repetition rate on the volume of material etched. Sinkovics established a MATLAB based model for explaining the thermal effects of laser ablation of polymers [27]. He assumed that the laser energy to heat transformation occurred instantly without any time. Balogh modeled the Nd:YAG laser ablation as a simple thermal process [28], the ablation threshold was set as a threshold temperature and the energy to temperature transformation factor. Experiments were performed on a polyimide film using a 355 nm and 300 μJ laser to validate the simulation results. Despite these extensive researches on laser ablation of polymers, the simulation and prediction based on laser ablation models are far from experimental conclusions [29]. The models available currently are established on some assumptions, such as neglecting the influence of incubation effect on the heating of the substrate, considering the ablation to happen only within a very thin surface layer [30, 31]. Further, different materials have intrinsic material properties, like thermal conductivity, absorption coefficient, etc. Therefore, currently, the models require frequent changes and alterations to predict the ablation process accurately.

In this thesis, we demonstrated a simple but effective approach to model micro-drilling process on polymer substrates using pulsed laser ablation. When a polymer substrate is identified, a process-based modeling procedure could be followed. This will help to predict the area-depth of blind micro-hole drilling based on experimental study results when the number of pulses and laser power is the two dominant factors in process control of laser ablation. A case study was conducted

where laser ablation of HDPE samples with 1064 nm laser was studied under different laser power and number of pulses. Simulation of the micro-drilling process was performed considering a purely thermal standpoint. A laser ablation model was established based on the experimental results, which adopted mathematical equations from the experimental observation to formulate a quantitative area-depth approximation model of the micro-drilled holes. The crater depths and diameters, observed using an optical 3D scanning microscope, were validated against the simulation results. The simulation model developed in this thesis has 96.5% accuracy for the area and 85.7% for the depth prediction on average. It will be a step and good example towards obtaining a quantitative depth-area approximation model that can be used widely on different polymer materials.

3.3 Experimental Setup and Results

Figure 3.1(a) represents the experimental setup for the micro-drilling. The topmost object in Figure 3.1(a) is the Opotek 3034 tunable laser head, which was operated at a constant wavelength of 1064nm. The diameter of the laser beam was 4mm, and the pulse duration was in the nanosecond regime. This laser light is represented by the red beam in Figure 3.1(a). It should be noted that in reality, this beam could not be seen as it operates in the infrared spectrum. The beam enters the focusing lens, which focuses the cylindrical beam into an ultra-small spot onto the sample. A Labmax PC laser power meter was used to measure the mean power of the laser at different energy percentages ranging from 10 to 100 percent. Figure 3.1(c) shows the power of the laser as a function of the percentage of maximum power. The maximum power of the laser system was 350 mW. The substrate material used was high-density polyethylene. The ablation threshold of HDPE is 38 J/cm^2 at 1064 nm wavelength. The high-density polyethylene (HDPE) sample, 0.4 mm thick, was mounted on a micro-positioning stage. It could vary the position in which the focused beam strikes the sample in the X and Y-axis. The Z-axis was kept constant as it was

calibrated such that the focused beam spot was as small as possible. The material of the micro-positioning stage used, was steel. All optical elements were arranged precisely to avoid errors in the system.
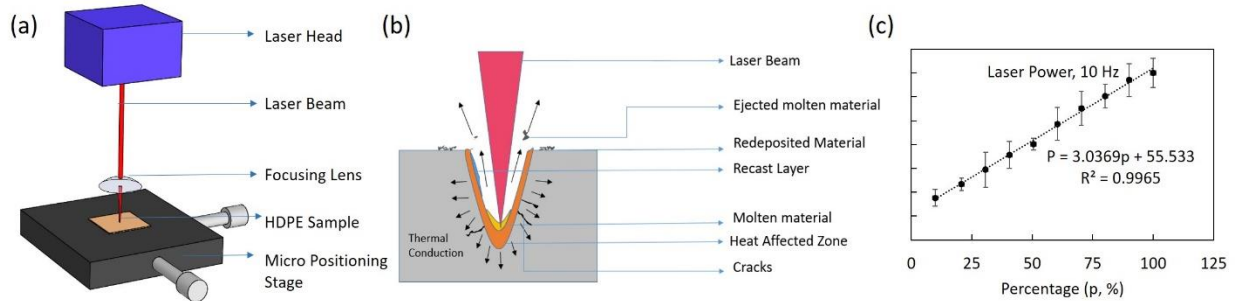

Figure 3.1 (a) Experimental setup of laser ablation: opotek 3034 tuneable laser at 1064 nm wavelength, (b) Mechanism of laser ablation, and (c) Laser power tuned at different percentages of maximum power.

The independent variables in the experiment were the power and the number of pulses, while the focal spot size, repetition rate, and wavelength were kept constant. The sample was irradiated for a combination of increased power and number of laser pulses. The number of laser pulses was varied from 3, 5, 7, 9, 11, 20, and 30 pulses. The pulse range was choses to show how the dimensions of the crater change with subsequent change in the number of pulses. The laser power was varied from 1, 3.3, 6.6, 10, 33, 66, and 100 percent. These ranges were chosen in order to have equal representation between the orders of magnitude. For example, 3.3 and 6.6 were chosen between 1 and 10, while 33 and 66 were chosen between 10 and 100. The power percentages were chosen to obtain data as a log of the input power. For each condition, the depth of ablation and the area of the ablated crater were observed and measured using a HiroxRH-2000 optical focus variation microscope. In this thesis study, the focus was more on to obtaining features in the micro scale with high aspect ratio. This was one of the reason why we focussed on the area and depth of the ablated crater and not the volume of the material removed or the rate at which the

material is removed. Figure 3.2(a-c) represents the dimensions of the crater and the 3D and 2D depth profile of the ablated hole captured by the optical 3D scanning microscope. It was observed that the obtained crater shape is more elliptical than circular. This could be due to human errors while clamping the substrate on the micropositioning stage and not having the laser beam strike perpendicular to the substrate. This could be due to the non uniformities on the HDPE sample that could have prevented the substrate from being placed flat on the stage. The area was calculated by fitting an ellipse to the observed crater shape and determining the major and minor axis length using the optical microscope, as shown in Figure 3.2(a). The mean depth of the hole was calculated based on 3D scanning results and cross-section profiles, as shown in Figure 3.2(b-c). The datum in Figure 3.2(b-c) is the bottom of the crater. The hole was generated with 5 pulses under 6.6% of maximum power, resulted in a ring outside the hole. It was the aggregation of melted materials during the ablation process. The measured data was then used to calculate the area of the elliptical shape crater.
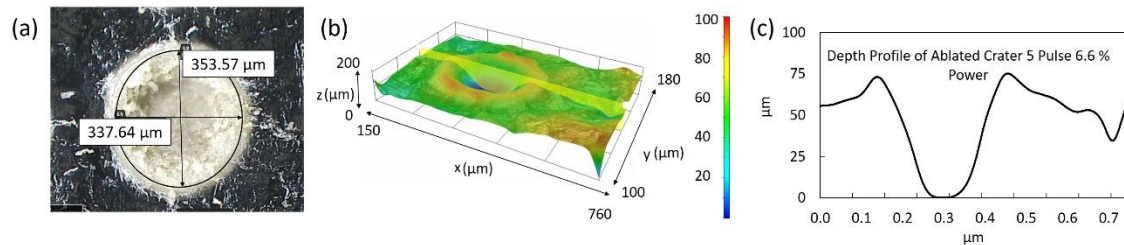

Figure 3.2 (a) 2D image of micro-drilled crater and (b) 3D profile of the micro-drilled hole, and (c) Cross sectional depth profile of micro-drilled hole for 5 pulses at 6.6% of maximum power

Figure 3.3(a-f) shows the 3D depth profile obtained from the optical microscope for 3, 7, 9, 11, 20, 30 pulses at 6.6 percentage power. With the increase of laser pulses, the depth of the hole becomes large. The amount of pulse affects the total energy applied to the polymer. Thus, different depths of the holes are generated with various pulses. All the independent variables were controlled via a computer to have maximum control and precision while reducing the possible

human errors. The power percentages were chosen to obtain data as a log function of the input power. The number of pulses was selected to show how a single pulse could affect the material and how additional pulses in a short time could change the depth and diameter of the ablated holes. All the ablation experiments and results measurements were taken on the optical table to ensure the stability of the system and precision of the data.
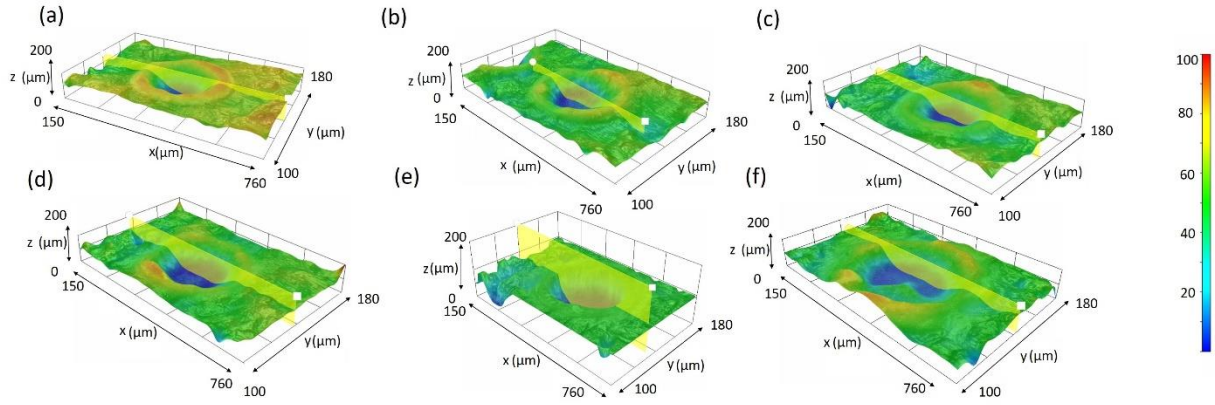

Figure 3.3 (a-f).3D profile of the micro-drilled holes for (a) 3, (b) 7, (c) 9, (d) 11, (e) 20, (f) 30 pulses and 6.6% of maximum power.

3.4 Data Analysis and Modelling

3.4.1 Effects of Number of Pulses and Power on Hole Depth

The hole depth as the function of the number of pulses and power percentage is shown in Figure 3.4(a-b), respectively. An overall upward trend in depth was observed along with an increase in power as well as an increase in the number of pulses. However, it can be seen that there was a relative decrease in depth at certain pulse numbers and power, which can be attributed to the presence of pores in the HDPE sample material or due to the non-uniform surface of the material used. The imperfection (e.g., pores in HDPE films) of substrate materials were intrinsic properties of the substrates that could not be controlled. However, due to the nature that all results came from substantial experimental data, one could consider the imperfection of the substrate as uncertainty that could be eliminated with enough data sampling. Another reason that could have resulted in

varying depth, could be heat transfer from the bottom of the substrate to the base plate of the micro positioning stage. The depth was modeled in a linear fashion, which was dependant on power along with the number of pulses. The depth equation was as follows.

$$D = ((-0.156 * LOG(P) + 3.4522) * N) + 21.573 * e^{(0.0034*P)} \tag{1}$$

Where D was the depth in µm, P was the power as a percentage (5 being 5%), and N being the number of pulses. The above equation was derived by plotting the experimental depth data obtained against power. The repetition rate in this experiment was 20 Hz, and the pulse duration was 10 ns.
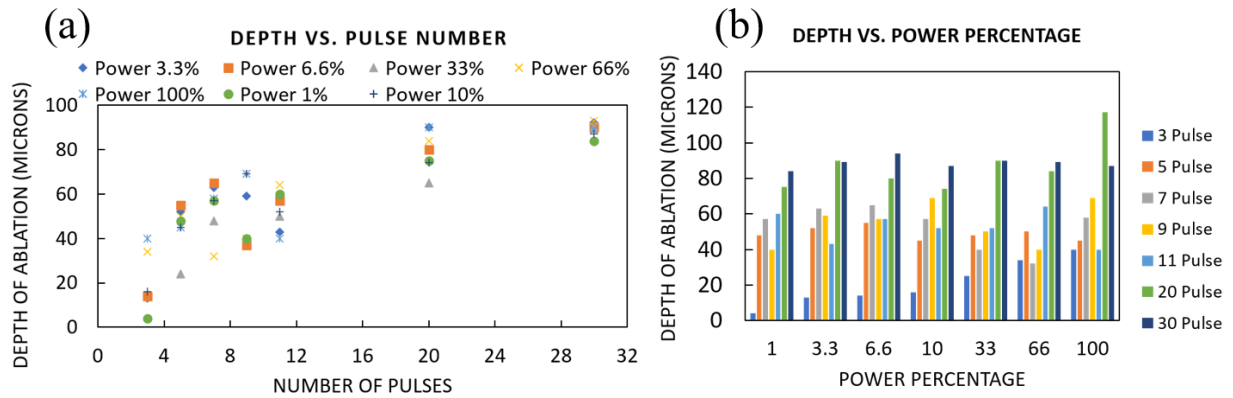

Figure 3.4 (a) Depth of ablation (µm) as a function of the number of pulses at several different power levels, and (b) Depth of ablation (µm) as a function of the power level at several different numbers of pulses.

The data also showed that a high depth of ablation could be achieved using low power, given that the number of pulses was high enough. The data showed that with lower percentage power with high number of pulses, the depth was higher than any other power percentage with maximum number of pulses, which indicated that it was possible to achieve a high depth of ablation with lower power by increasing the number of pulses. Under the power of 10%, the depth increased as the pulse number increase, seen in Figure 3.4(b). For laser ablation, it is essential to optimize both the number of pulses and laser beam power.

3.4.2 Effects of Number of Pulses and Power on Hole Area

The depth information can be coupled with the analysis of the area information. Unlike the depth information, the area demonstrated a clear trend, as shown in Figure 3.5(a), that was used to determine the area output as a function of the number of pulses and the power information. This is a characteristic of this particular system, but this general theory could be used for other materials after a simple characterization. The trend equation was as follows:

$$A = G_f * e^{(x *P)} = ((0.0033 * N) + 0.0728) * e^{(0.0062*P)} \tag{2}$$

where A represented the area of the ablation zone in mm^2, N represents the number of pulses and P represents the power as a percentage (100 being 100 percent). The equation mentioned above was derived from plotting the experimental area data obtained against the number of pulses. A gain factor was defined to represent the value by which the area of the crater increases for the subsequent steps in the number of pulses hitting the substrate. These gain factors were the values calculated from the exponential function in Figure 3.5(a). The equation of the trendlines from Figure 3.5(a) provided a gain factor $G_f = ((0.0033 * N) + 0.0728)$, shown in Figure 3.5(b). The gain factor was plotted against the pulse number, and an increasing linear trend can be observed. The equation generated from the trendline was used to determine the area of the ablated crater. This equation can be used to predict the area of ablated holes, which had an accuracy of 96.7%. The main contributor to the error between the trend line and the actual values was when the power was at 1%. The area observed was consistently lower than the predicted area. Further at certain experimental conditions with 1 percentage power, there was no material removal. Instead there was some material growth or changes on the exposed area. This could be due to thermal deformations occuring due to laser heating. It was important to note that a low power would result in a smaller area, but high pulses with low power could result in a large depth from the trend in

the number of pulses of Figure 3.4. This phenomenon indicated that a high aspect ratio could be achieved when using low power and large number of pulses, which was due to the fact that the increase in melt material caused by the increased power and the conduction of the heat through the material.
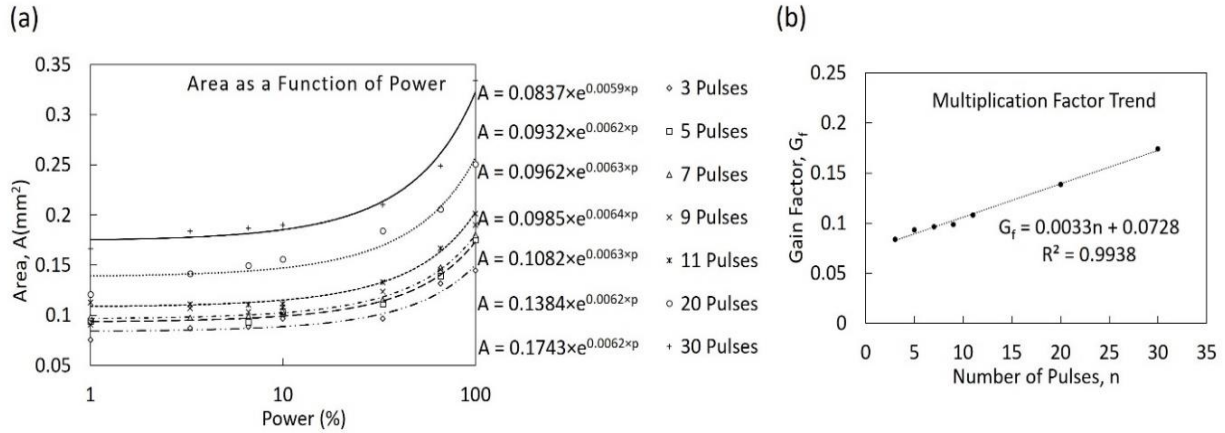

Figure 3.5 (a) Area as a function of the power for a given number of pulses, and (b) Multiplication factor trend used to calculate the area of the crater.

3.4.3 Area-Depth Approximation Model

The model based on the experiment data yielded depth and area information regarding the crater formed during the laser ablation process. The input parameters for this experiment were the pulse power as a percentage of maximum power, and the pulse number. With these, the area and depth were calculated using the equations above, which were derived from the data. There was no set equation to describe the depth and area of a crater for a given set of input parameters such as power and pulse number. In order to characterize this, trend lines were used to describe each set of independent variables.

The fits for these trend lines depended on the R^2 value. The smallest amount of deviation could always be obtained by using a high order polynomial fit, but it would not make logical sense for that trend. For example, the depth trend appeared to be linear, where the Y-intercept depended

on the power level. All of the lines had a similar slope, the trend line was then graphed, and it showed that this trend did indeed have the lowest R^2 value. As for the area, the data followed an exponential trend, showing that the area increases exponentially as the power of the laser increases. A line of best fit was then produced, and of the available fits, the exponential had the least deviation. The average percent error from the observed values of the area was 3.7%. Most of this deviation was a result of a larger area prediction for the 1% power pulses. This trend described how the additional power was translated into the heat and melting of the material.
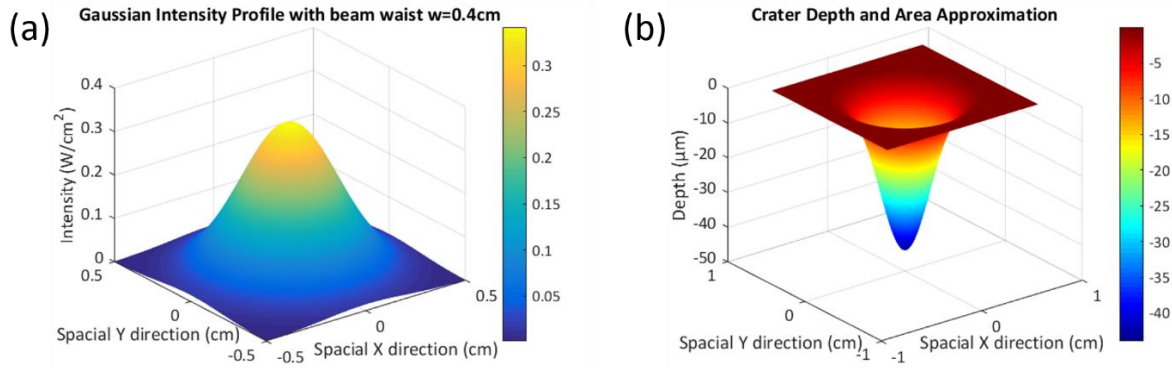

Figure 3.6 (a) Standard gaussian laser intensity profile for one individual pulse, and (b) Visual depiction of the area and depth of laser ablation zones at 5 pulses and 6.6% of max. power.

The laser profile on the surface follows the shape shown in Figure 3.6(a), which is a Gaussian beam, and the equation representing the Gaussian intensity is as follows:

$$I(r,z) = 2Pe^{\left(-\frac{2r^2}{w(z)^2}\right)} / \pi w \tag{3}$$

Where I is the intensity of the laser, P is the power, z is the propagation distance of the laser, r is the radius of the laser spot. The beam-width is characterized as the point at which the intensity drops to $1/e^2$ of the maximum intensity. In the case of the laser system in this study, the beam width was 4 mm. The power of the beam was measured and charactered using a power meter, and the result is the profile shown in Figure 3.6(b). These data points represented the average power over 10 seconds with a repetition rate of 10 Hz. From this, the peak power was characterized

and denoted as P in the equation. The power of the laser in this work resulted in the intensity distributions shown in Figure 3.6(a), which was just the fluence over 1 second. The fluence per pulse was the intensity over the repetition rate, which in this case, was 10. The fluence that resulted from this experiment was quite low. It led to additional melting instead of vaporization, resulting in smaller aspect ratios. Due to this beam profile, the ablation crater followed a similar shape, which was due to the relationship between the emitted energy and intensity. There was more energy in the middle of the pulse profile than the edge. The approximation of depth and area was characterized by the fits shown in Equation (1-2) and modeled in Figure 3.6(b). The crater shape was modeled using Euation 4. The normalization of the crater shape and establishing the depth was done by using Equation 5.

$$Crater = (2e^{\left(-\frac{2l^2}{w^2}\right)})/A \qquad (4)$$

$$Crater\ with\ depth = Crater \times D/\ \text{Maximum Value of Crater} \qquad (5)$$

Where l is the coordinates of the target plane, w is the beam width, A is the area, and D is the depth. The above two equations create the vector values of A and D to generate a series of values that indicate the profile of the hole. These values were then plotted against the x and y plane to obtain the visual representation of the area-depth approximation. Figure 3.7(a-b) represents the accuracy of the area and depth prediction of the quantitative approximation model comparing to experimental results, respectively. The depth-area approximation model was not 100% accurate due to two factors. The first factor, the top of the crater, has excess material that has been melted and expelled upwards. This material formed a ridge above the substrate surface, which was not consistent enough to characterize and model. This ridge can be viewed in Figure 3.2(b). This ridge formation can be the result of thermal deformation caused by the laser heating of the area around the target area. It can also be seen that the ridge was larger on the right side of the crater than the

left side, which was a typical example of the inconsistent ridge formation mentioned earlier. The second inconsistency was at the bottom of the ablation zone. The material was not completely expelled from the substrate, so there was a buildup at the bottom of the crater. This buildup filled in the bottom of the ablation zone, which caused the crater to have less depth and decreased the aspect ratio. The buildup at the bottom of the crater could be seen in Figure 3.2(b). This molten buildup was mostly due to the pulse duration of the nanosecond laser, which made the heat transfer to its surroundings and melted the material instead of vaporizing it. The buildup made it impossible to measure the "true" depth that the laser ablates as one could only measure to the top of the buildup. This was the reason that the predictive model appeared more narrow than an experimental profile. As a result of those inconsistencies, this model could be used to predict the area at the top of the crater, as well as the depth of the ablation zone. The shape profile differs in reality due to the excess molten material mentioned above. The model accuracy can be significantly enhanced when ablating through holes instead of blind holes. The area-depth approximation results of the simulation for various values of power percentage and pulse numbers were compared with the experimental observations. The percentage difference was calculated by using the difference between the experimental and simulation results divided by experimental results in the area and depth values. A difference value close to zero on the scale indicated a highly accurate prediction for that particular value of power and number of pulses. Figure 3.7(a-b) only demonstrated the total sampling points with the x-axis, indicating just a serial number of each sampling point.
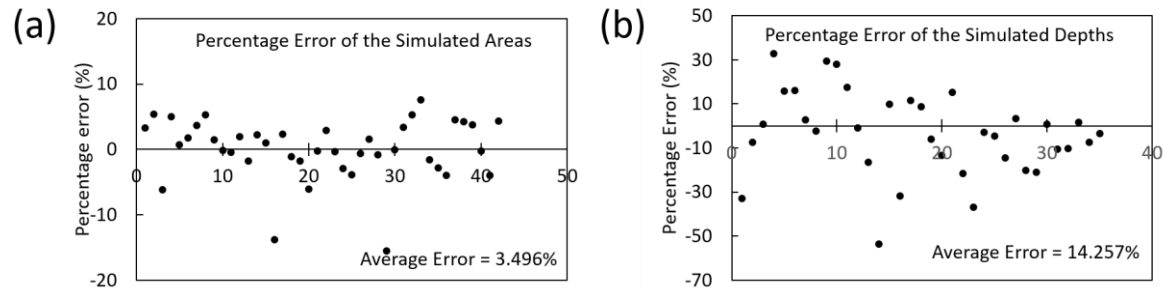
Figure 3.7 Accuracy of the (a) Area and (b) Depth approximation of the simulation with respect to the experimental observations.

The quantitative area-depth approximation model was developed by considering the laser drilling of the blind hole on HDPE soft films. This experimental based approach can be extrapolated for other materials by following the procedure described in Figure 3.8. The ablation was considered as a purely thermal process and began with defining the initial parameters of the laser. The target plane dimension and resolution are set, while a matrix was generated for the use in the calculation of the intensity of the laser. A surface plot has been created for the intensity values calculated at different points on the matrix, using the experimental peak power observed from the power meter. Similarly, the depth and the area of the drilled crater is determined from the experimental equations of depth approximation and gain factor trend. The values of depth and area of the drilled holes are normalized to create a surface plot prediction of the drilled hole. The accuracy of the model was represented by comparing the simulated values with the experimental data. This overarching approach could be powerful for rapid prototyping on new substrate materials using pulsed laser ablation, where the intrinsic properties of the substrate material cannot be acquired. It could also be integrated as a prediction and optimization tool for process engineers when micro-drilling using laser ablation.
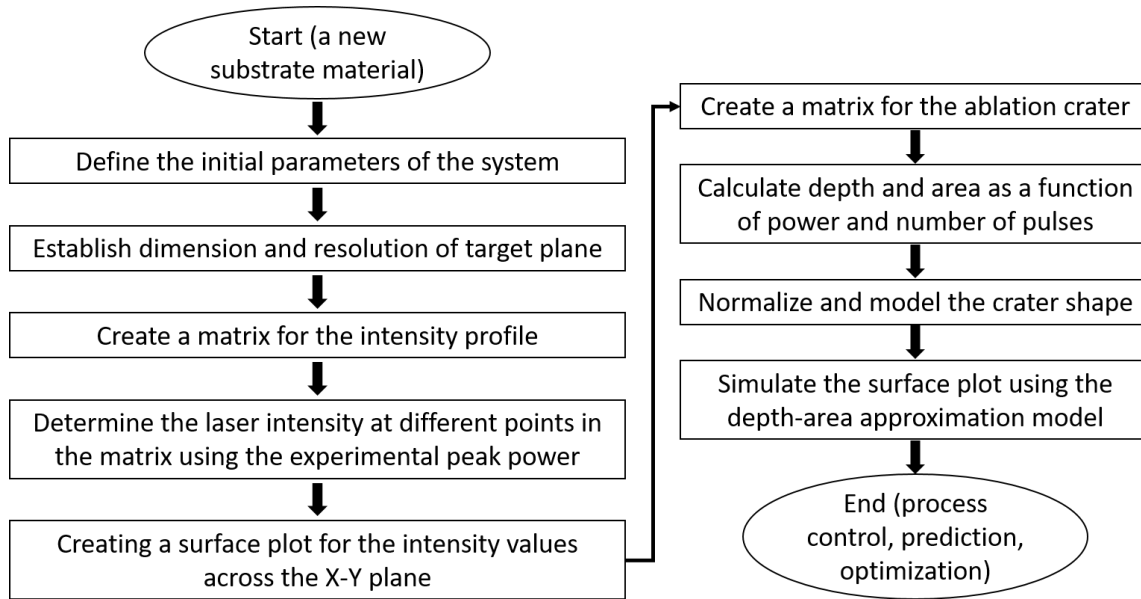
Start (a new substrate material)

Define the initial parameters of the system

Establish dimension and resolution of target plane

Create a matrix for the intensity profile

Determine the laser intensity at different points in the matrix using the experimental peak power

Creating a surface plot for the intensity values across the X-Y plane

Create a matrix for the ablation crater

Calculate depth and area as a function of power and number of pulses

Normalize and model the crater shape

Simulate the surface plot using the depth-area approximation model

End (process control, prediction, optimization)

Figure 3.8 Procedure to establish area-depth approximation model for micro-drilling based on pulsed laser ablation given any new substrate material.

3.5 Conclusion

A quantitative area-depth approximation model was developed to predict the area and depth of the micro-drilled holes based on experimental data. A purely thermal viewpoint was considered to model the laser ablation based micro-drilling. Micro-drilling was performed on high-density polyethylene (HDPE), and blind holes were fabricated by ablating under different number of pulses and laser power. An incremental trend was observed in the depth of the crater for an increase in the number of pulses and the laser power. The presence of pores in the HDPE sample and the non-uniform surface caused a relative decrease in depth of the micro-drilled holes. From the results, it was inferred that a higher aspect ratio could be achieved by decreasing the power and increasing the number of pulses. This also produced a lesser heat affected zone and melt expulsion crater. Gain factors were determined from the experimental area data and were used in simulating the area-depth approximation in the quantitative model. A comparison of the measured and simulated results yielded, on average, a 96.5% accuracy in predicting the area and 85.7%

accuracy in predicting the depth and is presented as a validation for the model. A sequential procedure used to establish the model has been presented, which will be a knowledge base for extending the model for other materials. This model will eliminate the time and material wastage involved in conducting test runs to determine the parameter settings required for producing a hole of specific dimensions. This model provides a simple but effective approach to predict dimensions of micro-holes on various substrates using laser ablation under different laser power and the number of pulses, which could pave the way for development and modeling of laser ablation on polymers.

Acknowledgment and Declaration of Interest

<div align="center">

3.6 Chapter 3: References

</div>

[1] Jiang, J., Callender,C.L.,Noad,J.P.,Walker,R.B.,Mihailov,S.J.Ding,.J.,&day,M. (2004);."All-polymer photonic devices using excimer laser micromachingning " IEEE Photonics Technology Letters, 16(2), 509-511.

[2] Naessens, K., Ottevaere, H., Baets, R., Van Daele, P., and Thienpont, H. (2003). "Direct writing of microlenses in polycarbonate with excimer laser ablation.(Author Abstract)," Applied Optics, 42(31), 6349.

[3] Pan, C. T., and Shen, S. C. (2004). "Design and fabrication of polymeric micro-optical components using excimer laser ablation," 20(2), 270-274.

[4] Hsieh, Y. K., Chen, S. C., Huang, W. L., Hsu, K. P., Gorday, K. A. V., Wang, T., and Wang, J. (2017) "Direct micromachining of microfluidic channels on biodegradable materials using laser ablation," Polymers, 9(7), 242.

[5] Klank, H., Kutter, J. P., and Geschke, O. (2002). "CO2-laser micromachining and back-end processing for rapid production of PMMA-based microfluidic systems," Lab on a Chip, 2, 242-246.

[6] Lan, B., Hong, M. H., Ye, K. D., Chen, S. X., and Chong, T. C. (2003). "Laser ablation for MEMS microfabrication on Si and Kapton substrates," In Third International Symposium on Laser Precision Microfabrication, 4830, 196-201.

[7] Shin, B. S., Oh, J. Y., and Sohn, H. (2007). "Theoretical and experimental investigations into laser ablation of polyimide and copper films with 355-nm Nd:YVO4 laser," Journal of Materials Processing Technology, 187, 260-263.

[8] Dyer, P. E., and Sidhu, J. (1985). "Excimer laser ablation and thermal coupling efficiency to polymer films," Journal of Applied Physics, 57(4), 1420-1422.

[9] Lippert, T., Hauer, M., Phipps, C. R., and Wokaun, A. (2003). "Fundamentals and applications of polymers designed for laser ablation," Appl Phys A, 77(2), 259-264.

[10] LaHaye, N. L., Harilal, S. S., Diwakar, P. K., Hassanein, A., and Kulkarni, P. (2013). "The effect of ultrafast laser wavelength on ablation properties and implications on sample introduction in inductively coupled plasma mass spectrometry," Journal of Applied Physics, 114(2), 023103.

[11] Aguiar, R., Trtik, V., Sánchez, F., Ferrater, C., and Varela, M. (1997). "Effects of wavelength, deposition rate and thickness on laser ablation deposited YSZ films on Si(100)," Thin Solid Films, 304(1), 225-228.

[12] Burns, F. C., and Cain, S. R. (1996). "The effect of pulse repetition rate on laser ablation of polyimide and polymethylmethacrylate-based polymers," Journal of Physics D: Applied Physics, 29(5), 1349-1355.

[13] Chichkov, B. N., Momma, C., Nolte, S., Von Alvensleben, F., and Tünnermann, A. (1996). "Femtosecond, picosecond and nanosecond laser ablation of solids," Applied Physics A: Materials Science and Processing, 63(2), 109-115.

[14] Johnson, S. L., Schriver, K. E., Haglund, R. F., and Bubb, D. M. (2009). "Effects of the absorption coefficient on resonant infrared laser ablation of poly(ethylene glycol)," Journal of Applied Physics, 105(2), 024901.

[15] Pham, D., Tonge, L., Cao, J., Wright, J., Papiernik, M., Harvey, E., and Nicolau, D. (2002). "Effects of polymer properties on laser ablation behaviour," Smart Materials and Structures, 11(5), 668.

[16] Benavides, O., de La Cruz May, L., Flores Gil, A., and Lugo Jimenez, J. A. (2015). "Experimental study on reflection of high-intensity nanosecond Nd:YAG laser pulses in ablation of metals," Optics and Lasers in Engineering, 68, 83-86.

[17] Benavides, O., Golikov, V., and Lebedeva, O. (2013). "Reflection of high-intensity nanosecond Nd:YAG laser pulses by metals," Applied Physics A: Materials Science and Processing, 112(1), 113-117.

[18] Küper, S., and Stuke, M. (1987). "Femtosecond UV excimer laser ablation," Applied

Physics B, 44(4), 199-204.

[19] Misra, A., Mitra, A., and Thareja, R. K. (1999). "Diagnostics of laser ablated plasmas using fast photography," Applied Physics Letters, 74(7), 929-931.

[20] Bogaerts, A., Chen, Z., Gijbels, R., and Vertes, A. (2003). "Laser ablation for analytical sampling: what can we learn from modeling?," Spectrochimica Acta Part B: Atomic Spectroscopy, 58(11), 1867-1893.

[21] Cummings, J. P., and Walsh, J. T. (1993). "Erbium laser ablation: The effect of dynamic optical properties," Applied Physics Letters, 62(16), 1988-1990.

[22] Nayak, N. C., Lam, Y. C., Yue, C. Y., and Sinha, A. T. (2008). "CO2-laser micromachining of PMMA: The effect of polymer molecular weight," Journal of Micromechanics and Microengineering, 18(9), 095020.

[23] Wang, W., Mei X., Jiang, G.,Lei,S.,&Yang C (2008). "Effect of two typical focus positions on microstructure shape and morphology in femtosecond laser multi-pulse ablation of metals," Applied Surface Science, 255(5), 2303-2311.

[24] Tawfik, W., Farooq, W. A., and Alahmed, Z. A. (2014). "Damage Profile of HDPE Polymer using Laser-Induced Plasma," Journal of the Optical Society of Korea, 18(1), 50-54.

[25] Torrisi, L., Gammino, S., Mezzasalma, A. M., Visco, A. M., Badziak, J., Parys, P., Wolowski, J., Woryna, E., Krása, J., Láska, L., Pfeifer, M., Rohlena, K., and Boody, F. P. (2004). "Laser ablation of UHMWPE-polyethylene by 438 nm high energy pulsed laser," Applied Surface Science, 227(1), 164-174.

[26] Gordon, P., Balogh, B., and Sinkovics, B. (2007). "Thermal simulation of UV laser ablation of polyimide," Microelectronics Reliability, 47(2), 347-353.

[27] Sinkovics, B., Gordon, P., and Harsányi, G. (2010). "Computer modeling of the laser ablation of polymers," Applied Thermal Engineering, 30(16), 2492-2498.

[28] Balogh, B., Gordon, P., and Sinkovics, B. (2006). "Description of 355 nm laser ablation of polyimide as a thermal process," 2006 1st Electronic Systemintegration Technology Conference, IEEE, 360-364.

[29] Bityurin, N., Luk'Yanchuk, B. S., Hong, M. H., and Chong, T. C. (2003). "Models for Laser Ablation of Polymers," ChemInform, 103(2), 519-552.

[30] Arnold, N., Luk'Yanchuk, B., and Bityurin, N. (1998). "A fast quantitative modelling of ns laser ablation based on non-stationary averaging technique," Applied Surface Science, 129, 184-192.

[31] Luk, Amp, Apos, Yanchuk, B., Bityurin, N., Himmelbauer, M., and Arnold, N. (1997). "UV-laser ablation of polyimide: from long to ultra-short laser pulses," Nuclear Inst. and Methods in Physics Research, B, 122(3), 347-355.

CHAPTER 4.   FINITE ELEMENT METHOD (FEM) BASED SIMULATION OF LASER ABLATION: SURFACE TEMPERATURE AND DEPTH PROFILE EVOLUTION

Modified from a manuscript accepted for publication in the 2020 Manufacturing Science & Engineering Conference Proceeding.

Sandeep Ravi-Kumar[a] , Liangkui Jiang[a], Hantang Qin[a]

[a]*Industrial and Manufacturing Systems Engineering, Iowa State University, Ames, IA 50011*

USA

In addition to the quantitative model presented in Chapter 3, I have developed a finite element based simulation model that can predict the ablation surface temperature and the depth profile evolution during laser ablation. This model was aimed to provide a better understanding of the ablation threshold conditions and the initiation of ablation. I have contributed to more than 70% of the work in this chapter. The work presented in this thesis chapter has been accepted for publication in the "2020 Manufacturing Science and Engineering Conference Proceedings."

4.1 Abstract

Laser ablation has been widely used for material removal on different types of substrates. Accurate feature profile fabrication with minimum damage to the surrounding material requires precise control of the laser and material parameters. One approach to achieve this is by establishing a simulation model to help process control and optimization. However, laser ablation is a complex process that is difficult to model. In this chapter, numerical simulation models have been established to identify the temperature at the ablation surface and the ablation depth profile evolution over time. The ablation has been modeled using the heat transfer in solids module in COMSOL Multiphysics with the manual material definition of high-density polyethylene (HDPE). The laser beam is modeled as a continuous heat source by utilizing a ramp function. Information

for establishing a pulsed laser system has been provided. Results are provided for the surface temperature and depth profile evolution for various time steps. Results of the simulation of laser ablation of the HDPE sample using a 50W laser using both the models were presented. The next step of our work is to validate the simulation results by comparing it against experimental data. This will render these models to have the potential to be able to predict the ablation crater profile with higher accuracy. This model will pave the way for a better understanding of the ablation threshold conditions and identifying the ablation initiation in any material, given the material properties are known.

4.2 Introduction

Laser ablation (LA), also known as photo-ablation, is the process of removing material by irradiating it with a laser beam [1-2]. As a rapid manufacturing approach in the industry, it has been employed to remove many kinds of materials, such as polymers [3-4], metals [5], ceramics [6], and semiconductors [7], even biological tissues [8]. During the ablation process, materials are removed by a high-power laser beam, leaving holes or desired patterns. The laser flux affects the material conditions. The material is heated by the absorbed laser energy and evaporates at low laser flux, while the material is typically converted to a plasma at high laser flux. Compared with the traditional manufacturing methods of micro-nano materials, LA has several advantages: (i) it is a rapid and high-efficiency approach to manufacture designed structures without masks. Thus, complicated structures are generated by LA [9-11]. (ii) LA is a chemically clean, simple, and straightforward method with almost all kinds of materials and solvents from metals to polymers. With different laser beam, liquid and solid materials are both ablated into designed patterns. (iii) The ablation process is mild without any particular temperature and pressure requirements, which results in broad application scope in industrial manufacturing. (iv) There are different lasers that

are employed for ablation, including nanosecond laser [12], femtosecond laser [13], and picosecond laser [14]. These lasers are used in special kinds of materials, resulting in the synthesis of micro-nano structures in one-step or multi-step.

The nature of LA is the interaction between laser and matter, which generates a thermal effect on materials. Mafuné [15] reported the fabrication of silver nanoparticles by laser ablation of a metal silver plate in an aqueous solution, which showed almost the same absorption spectrum as the chemistry method fabrication. McCann [16] reported the fabrication of microchannel on cyclic olefin polymer films using a picosecond pulsed 1064 nm Nd: YAG laser. It showed an excellent ability to tailor microchannel depth and width by varying laser fluence. Many optical devices were also realized by LA, such as parallel surface gratings and Fresnel zone plates [17]. For composites material, Taki [18] reported a micro square grid fabricated on an aluminum surface using LA by introducing molten glass-reinforced poly(butylene terephthalate), poly(styrene) and acrylonitrile–butadiene–styrene, which has excellent mechanical property. A novel sensor patch was developed by polyethylene terephthalate films metalized with aluminum. This tactile sensor showed promising results for using these patches in applications with contact pressures considerably lesser than normal human contact pressure [19]. LA is now widely used in manufacturing nanoparticles, optical devices, biological sensors, and other functional structures.

It is still not fully clear for the mechanism of LA, especially the interactions of laser and matter. The researchers paid much attention to the simulation and theoretical analysis of LA. In 1965, Ready [20] proposed two models and analyzed the effects of high-power pulses of laser radiation of specified shapes absorbed at opaque surfaces. Chan [21] reported a one-dimensional steady-state model to describe the damage caused by materials removal by vaporization and liquid expulsion by a Mott-Smith-type solution. García [22] presented a detailed study of the wavelength

influence in pulsed laser annealing of amorphous silicon thin films with UV (355 nm), visible (532 nm) and IR (1064 nm), and KrF (248 nm) excimer laser sources. Strop [23] established a 3D axisymmetric finite element model to simulate the process of LA. It showed that irradiation of the molybdenum layer with an ultra-short pulse caused a rapid acceleration in the direction of the surface normal within a time frame of a hundred picoseconds to a peak velocity of about 100 m/s. Zhang [24] proposed a thermal physics model of continuous-wave laser melting of germanium epitaxial films on silicon substrates in COMSOL Multiphysics based on heat transfer theory. In previous works, the simulation of LA was focused on different models with potential application areas and conventional materials.

There are still many limitations of the polymer-based LA model to analyze the ablated structures with the relationship of laser parameters. In this thesis chapter, we proposed two models of thermal laser ablation by a continuous laser system using COMSOL Multiphysics that helps determine the temperature at the ablation surface and the depth of ablation. The heat transfer module was used with a manual material definition to establish an HDPE sample. This work could promote the development of polymer-based LA and provide an effective way of determining the initiation of ablation.

4.3 Materials and Methods
4.3.1   Simulation Model

Assumptions were made in order to simplify this model of laser ablation and are as follows.

1. The ablation is a purely thermal process. No chemical reaction influence is taken into consideration.

2. The ablation model is only suitable for materials that undergo sublimation.

3. The phase change occurs only on the top surface, and no internal heating occurs. Thus, we eliminate the chances of gas-filled voids forming under the substrate material leading to cavitation.

4. The material properties remain unaffected by the temperature changes of the substrate.

5. The gaseous material formed is removed immediately. There is no interaction between the removed material and the laser beam. So, the heating of the substrate by the upcoming laser beam is not affected by the gaseous plume formed.

6. Radiative heat transfer does not occur during the ablation process.

4.3.2 Laser Procedure

The laser beam was modeled as a heat source acting on a plane. The laser power is set as 50W with a spot radius of 2mm. The laser heat source is applied in the form of a ramp function with a slope of 10^9, as shown in Figure 4.1. This function helps depict the heat source as a continuous laser system. This ramp function establishes the temperature-dependent heat transfer coefficient required to model the ablative heat flux.
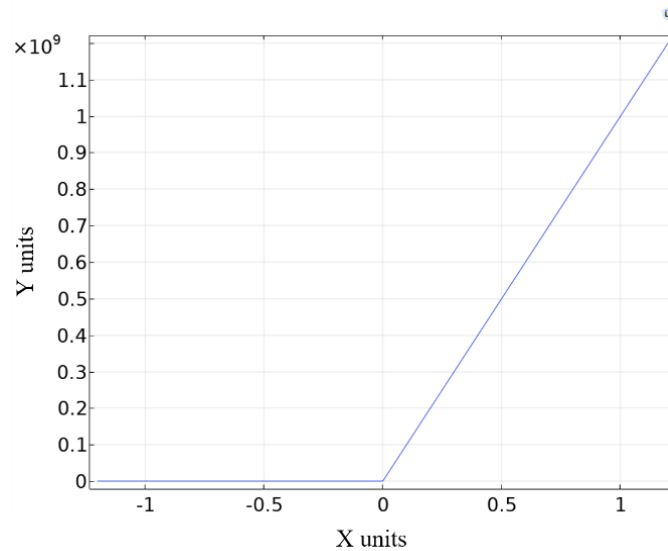

Figure 4.1 Ramp function.

A pulsed laser system can also be modeled by multiplying the heat flux with an analytic function provided in the COMSOL library that represents the frequency of pulses hitting the substrate, as shown in Figure 4.2.
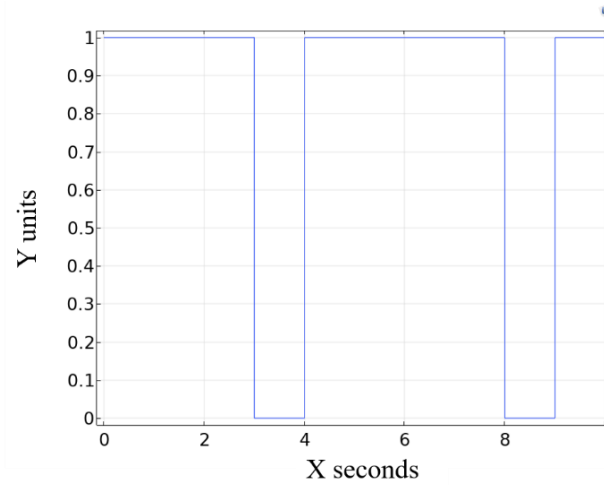

Figure 4.2 Analytic function that can depict a pulsed laser system.

4.3.3 Geometric Description of the Model

The HDPE sample is modeled as a two-dimensional rectangle of width and height of 5cm for the depth model and as a cuboid with a thickness of 1cm for the surface temperature model. The depth model has been established in two dimensions since we do not consider the diameter of the ablated crater in this simulation. The ambient environmental conditions are set at 293.15K temperature and 1-atmospheric pressure. Table 4.1 represents the material properties used for defining the sample in the simulation of laser ablation. These properties are derived from the previous research works and best judgement. There might be some discrepancies between the material properties provided in this section to the actual material properties of HDPE.

Table 4.1. Material properties used in COMSOL simulation.

Property	Expression	Value
Thermal Conductivity	K	0.48 W/m-K
Density	P	975 kg/m^3
Specific Heat Capacity	C_p	1000 J/kg-K
Heat of Sublimation	Hs	500 kJ/kg

Since we assume that the ablation and the heating are only occurring at the top surface of the sample, a user-defined free triangular and tetrahedral mesh has been established, as shown in Figures 4.3(a-b). This allows for more accurate finite element simulations at the laser-matter interaction zone and minimizes the time spent for calculations beneath the top layer.
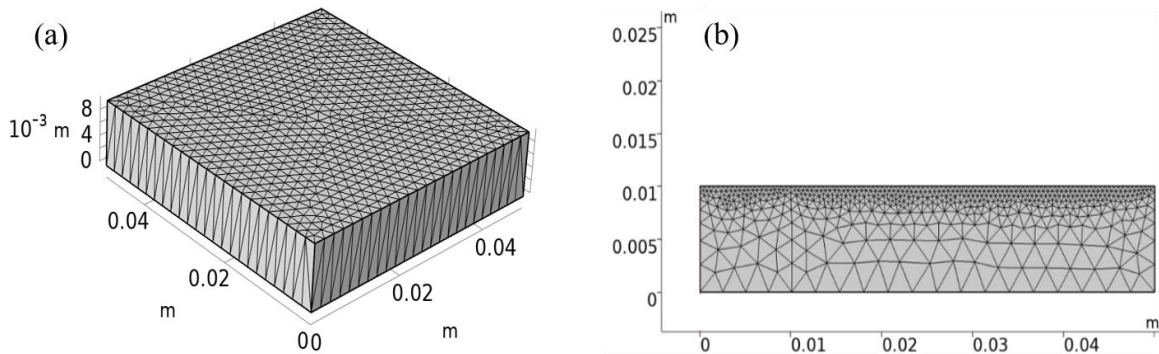

Figure 4.3 Mesh geometry for (a) surface temperature model (b) depth model.

4.3.4   Heat Transfer Description

The thermal boundary condition for the laser ablation models involves the heat flux to be applied at the top surface of the system. The remaining surfaces are provided with thermal insulation. A general inward heat flux (q_i) is applied on the top surface of the HDPE sample. In order to represent the laser ablation, an ablative heat flux, which is a convective heat flux and is

established on the top surface of the rectangular sample. Equation 1 represents the ablative heat flux provided using the COMSOL heat transfer is the solids module.

$$q_a = h(T - T_a) \qquad (1)$$

Where q_a is the ablative heat flux, T is the temperature of the substrate at any given time, T_a is the temperature at which ablation initiates, and h is the temperature-dependent heat transfer coefficient. In this thesis work, this temperature-dependent heat transfer coefficient is established using the ramp function, as shown in Equation 2. This means that the heat transfer coefficient is zero before the start of ablation and increases linearly after the ablation initiates.

$$h = Ramp(T - T_a) \qquad (2)$$

Where Ramp represents the ramp function, as shown in Figure 4.1. To represent the material being removed during the ablation, the deformed geometry interface in COMSOL has been employed. It has been established that the velocity of ablation is independent of the absorption coefficient and is influenced by the power density of the material [25]. Equation 3 governs the ablation rate of the substrate.

$$V = \frac{q}{\rho H_s} \qquad (3)$$

Where V is the ablation velocity, ρ is the density of the material, and H_s is the heat of sublimation temperature. This material removal rate is established in the COMSOL model by setting the prescribed normal mesh velocity as the above equation. The term q in Equation 3 is cumulative of the two heat flux established in the model.

4.4 Simulation Results

The simulation was finished using the time-dependent solver setting in COMSOL. The computation was done for a time duration of 60 seconds, with 0.1 second time steps. Figures 4.4 and 4.5 represent the results of the surface temperature model at 3 and 4 seconds, respectively.
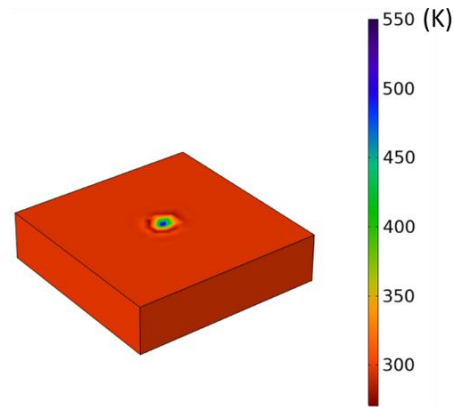

Figure 4.4 Temperature distribution in Kelvin across the surface at time 3 seconds.
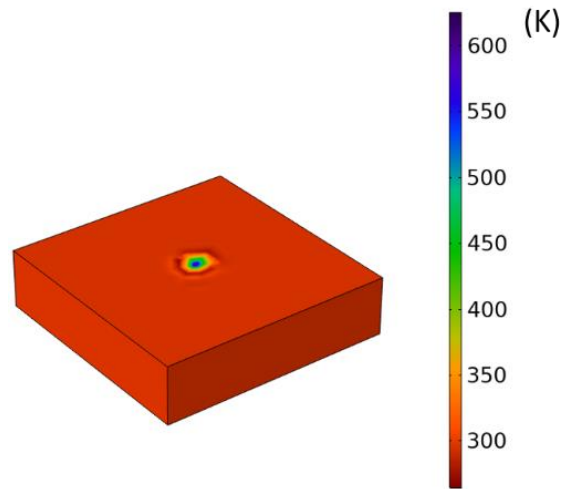

Figure 4.5 Temperature distribution in Kelvin across the surface at time 4 seconds.

From the simulation, temperature information was gathered at various times during the laser ablation process. A graph was plotted for the laser spot temperature against time steps, as shown in Figure 4.6.
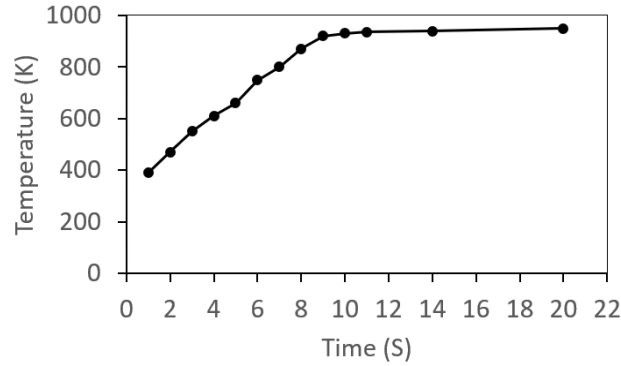
Figure 4.6 Surface temperature at the laser spot vs. time steps during laser ablation using 50w laser at 0.002m spot radius.

It was observed that the surface temperature due to ablative laser heating increases gradually over time and then saturates at 900K. Similar to the temperature model, the depth model was also solved using the time-dependent solver in COMSOL. Figure 4.7 represents the ablation profile evolution over time. The results also represent the heat-affected zones created during the ablation of the substrate.

It was observed from the depth model that the ablation started at 5.6 seconds, and the depth gradually increased over time. There are several benefits to these simulations. From these results, the user can identify the time at which the ablation initiates for a given laser fluence value. Meanwhile, the user can benefit by identifying the surface temperature at which the ablation starts. Traditionally, the laser ablation threshold is mentioned in terms of ablation threshold fluence, which means the amount of laser energy required to initiate ablation. However, over time, the heat accumulation on the surface of the material results in ablation to occur at fluences below the ablation threshold fluence. In conclusion, this model will help researchers determine the threshold condition in terms of temperature, irrespective of the laser fluence.
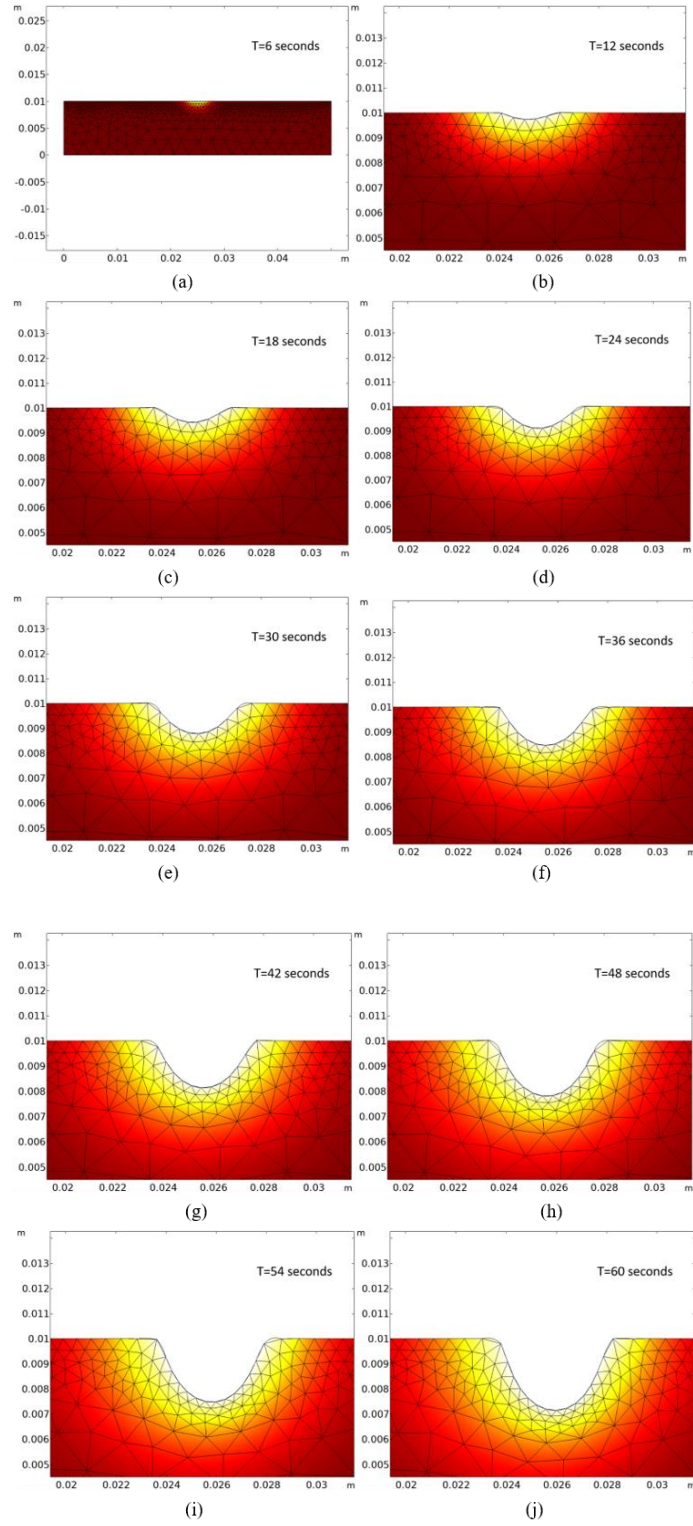
Figure 4.7 Heat affected zones at different laser ablation time.

4.5 Future Work

The next step in this model is to validate the simulation results by comparing it against experimental data. This will render these models to have the potential to be able to predict the ablation crater profile with accuracy, provided the material properties are known. Discrepancies in the material property might cause variations in the predicted results. So, validation of this model could be performed based on a material with very well-defined material properties. Also, improvements will be made by taking into consideration some of the assumptions that were neglected in the current models. For example, the future model will take into consideration the effect of the interaction of the removed material with the upcoming laser beam, radiative heat transfer in the material, and temperature-dependent material properties.

4.6 Conclusion

In this chapter, numerical models were established that predict the ablation surface temperature and the evolution of the ablated profile using a heat transfer module in COMSOL. The material was manually defined to be a high-density polyethylene sample with isotropic properties. The laser beam was modeled as a continuous heat source. Information on how to establish a pulsed laser system has been provided. Results of the simulation of laser ablation of the HDPE sample using a 50W laser using both the models were presented. This model will pave the way for a better understanding of the ablation threshold conditions and identifying the ablation initiation in any material, given the material properties are known.

Acknowledgments

4.7 Chapter 4: References

[1] Chichkov BN, Momma C, Nolte S, Von Alvensleben F, Tünnermann A. (1996). Femtosecond, picosecond and nanosecond laser ablation of solids. J Applied Physics A.; 63(2):109-15.

[2] Ravi-Kumar S, Lies B, Zhang X, Lyu H, Qin H. (2019). Laser ablation of polymers: a review. Polymer International. 68(8):1391-1401.

[3] Srinivasan R. (1986). Ablation of polymers and biological tissue by ultraviolet lasers. Science. 234(4776):559-65.

[4] Ravi-Kumar S, Zhang X, Lies B, Jiang L, Qin H. (2019). An Area-Depth Approximation Model of Microdrilling on High-Density Polyethylene Soft Films Using Pulsed Laser Ablation. Journal of Micro and Nano-Manufacturing. 7(4): 044501.

[5] Nolte S, Momma C, Jacobs H, Tünnermann A, Chichkov BN, Wellegehausen B, et al. (1997). Ablation of metals by ultrashort laser pulses. J JOSA B. 14(10):2716-22.

[6] Ihlemann J, Scholl A, Schmidt H, Wolff-Rottke B. (1995). Nanosecond and femtosecond excimer-laser ablation of oxide ceramics. Applied Physics A. 60(4):411-7.

[7] Morales AM, Lieber CM. (1998). A laser ablation method for the synthesis of crystalline semiconductor nanowires. Science. 279(5348):208-11.

[8] Vogel A, Venugopalan V. (2003). Mechanisms of pulsed laser ablation of biological tissues. J Chemical reviews. 103(2):577-644.

[9] Pronko PP, Dutta SK, Squier J, Rudd JV, Du D, Mourou G. (1995). Machining of sub-micron holes using a femtosecond laser at 800 nm. Optics communications. 114(1-2):106-10.

[10] Stoian R, Rosenfeld A, Ashkenasi D, Hertel IV, Bulgakova NM, Campbell EEB. (2002). Surface charging and impulsive ion ejection during ultrashort pulsed laser ablation. Physical review letters. 88(9):097603.

[11] Nakata Y, Okada T, Maeda M. (2002). Fabrication of dot matrix, comb, and nanowire structures using laser ablation by interfered femtosecond laser beams. Applied physics letters. 81(22):4239-41.

[12] Camacho JJ, Oujja M, Sanz M, Martínez-Hernández A, Lopez-Quintas I, de Nalda R, et al. (2019). Imaging spectroscopy of Ag plasmas produced by infrared nanosecond laser ablation. J Anal Atom Spectrom. 34(3):489-97.

[13] Liao C, Anderson W, Antaw F, Trau M. (2018). Maskless 3D ablation of precise microhole structures in plastics using femtosecond laser pulses. ACS Appl Mater Inter. 10(4):4315-23.

[14] Jandeleit J, Urbasch G, Hoffmann HD, Treusch HG, Kreutz EW. (1996). Picosecond laser ablation of thin copper films. Applied Physics A. 63(2):117-21.

[15] Mafuné F, Kohno J-y, Takeda Y, Kondow T, Sawabe H. (2000). Formation and size control of silver nanoparticles by laser ablation in aqueous solution. The Journal of Physical Chemistry B. 104(39):9111-7.

[16] McCann R, Bagga K, Groarke R, Stalcup A, Vázquez M, Brabazon D. (2016). Microchannel fabrication on cyclic olefin polymer substrates via 1064 nm Nd: YAG laser ablation. Appl Surf Sci. 387:603-8.

[17] Zhao Q, Yetisen AK, Sabouri A, Yun SH, Butt H. (2015). Printable nanophotonic devices via holographic laser ablation. ACS nano. 9(9):9062-9.

[18] Taki K, Nakamura S, Takayama T, Nemoto A, Ito H. (2016). Direct joining of a laser-ablated metal surface and polymers by precise injection molding. Microsystem Technologies. 22(1):31-8.

[19] Nag A, Mukhopadhyay SC, Kosel J. (2016). Tactile sensing from laser-ablated metallized PET films. IEEE Sensors Journal. 17(1):7-13.

[20] Ready JF. (1965). Effects due to absorption of laser radiation. Journal of Applied Physics. 36(2):462-8.

[21] Chan CL, Mazumder J. (1987). One-dimensional steady-state model for damage by vaporization and liquid expulsion due to laser-material interaction. Journal of Applied Physics. 62(11):4579-86.

[22] García O, García-Ballesteros JJ, Munoz-Martin D, Núñez-Sánchez S, Morales M, Carabe J, et al. (2012). Estimation of Local Crystallization of a-Si:H Thin Films by Nanosecond Pulsed Laser Irradiation Through Local Temperature Simulation. Physics Procedia. 39:286-94.

[23] Sotrop J, Kersch A, Domke M, Heise G, Huber HP. (2013). Numerical simulation of ultrafast expansion as the driving mechanism for confined laser ablation with ultra-short laser pulses. Applied Physics A. 113(2):397-411.

[24] Zhang J, Song J, Liu Z, Hao X, Chen H, Hu H, et al. (2017). Modeling of continuous wave laser melting of germanium epitaxial films on silicon substrates. Materials Express. 7(5):341-50.

[25] Gijsbers, G. H., Selten, F. M., & van Gemert, M. J. (1991). CW laser ablation velocities as a function of absorption in an experimental one-dimensional tissue model. Lasers in surgery and medicine, 11(3), 287-296.

CHAPTER 5.   GENERAL CONCLUSION

Laser ablation has achieved a considerable amount of research attention in terms of the fabrication of micro/nano structures on polymer materials. In this thesis, an extensive literature review on polymer laser ablation was presented to understand the effect of laser parameters on machining, their influence on the substrate's surface morphology, and the various applications of laser ablation. Different laser types and influences of laser parameters to ablated polymeric structures have also been presented. This extensive literature review was published as a review paper titled "Laser Ablation of Polymers: A Review" in the journal "Polymer International." The journal publication is available in this link (https://doi.org/10.1002/PI.5834).

Secondly, experiments were conducted on laser ablation based micro-drilling of blind holes on High-density polyethylene samples using 1064 nm laser at various pulse numbers and laser power to determine its impact on the dimensions of the holes. It was evident that an increased aspect ratio feature can be produced by lowering the laser power and increasing the number of pulses. This condition also seemed to decrease the heat-affected zone and melt expulsion craters. Gain factors were determined from the trends plotted and were used to develop a quantitative area depth approximation model of laser ablation to predict the area and depth of micro-drilled holes. The developed model was validated against experimental area-depth data and yielded an average of 96.5%, and 85.7% accuracy in predicting the area and the depth of the micro-drilled holes on HDPE, respectively. Additionally, the procedure adopted in establishing this model was presented for it to act as a knowledge base for the future. This work has been peer-reviewed and published in "Journal of Micro and Nano-manufacturing" titled "An Area-Depth Approximation Model of Micro-drilling on High-Density Polyethylene Soft Films Using Pulsed Laser Ablation." The journal publication is available in this link (https://doi.org/10.1115/1.4045331).

Additionally, the finite element method-based model has been developed to predict the ablation surface temperature and the depth profile evolution over time. The model was established in the COMSOL Multiphysics with heat transfer in solids module. The laser source was defined as a continuous heat source, and the material properties were manually defined as HDPE. The results from this simulation model help in a better understanding of the ablation threshold and the initiation of ablation in terms of ablation threshold temperature. This works has been accepted for publication in the "2020 Manufacturing Science & Engineering Conference Proceedings."

The future scope of this thesis work would be to validate the current FEM based model against experimental results. Furthermore, the FEM based simulation model can be converted into a more sophisticated model of laser ablation by taking temperature-dependent material properties into consideration. Another aspect is to consider the interaction between ablation debris and plasma plume with the subsequent incoming laser pulses and validating it with experimental data.